Structural and metamorphic evolution during rapid exhumation in the Lepontine dome (southern Simano and Adula nappes, Central Alps, Switzerland)

Autor(en): **Nagel, Thorsten / Capitani, Christian de / Frey, Martin**

Objekttyp: **Article**

Zeitschrift: **Eclogae Geologicae Helvetiae**

Band (Jahr): **95 (2002)**

Heft 3

PDF erstellt am: **21.07.2024**

Persistenter Link: https://doi.org/10.5169/seals-168962

0012-9402/02/030301-21
Birkhäuser Verlag, Basel, 2002

Eclogae geol. Helv. 95 (2002) 301–321

Structural and metamorphic evolution during rapid exhumation in the Lepontine dome (southern Simano and Adula nappes, Central Alps, Switzerland)

THORSTEN NAGEL[1], CHRISTIAN DE CAPITANI[2], MARTIN FREY[3], NIKOLAUS FROITZHEIM[1], HOLGER STÜNITZ[2] & STEFAN M. SCHMID[2]

Key words: Central Alps, Adula Nappe, exhumation, decompression, high-pressure metamorphism

ABSTRACT

The three main deformation phases recorded in the southern Simano and Adula nappes are all associated with decompression at high temperatures above 600 °C. Deformation related to the Zapport phase (local D1) took place between 40 and 35 Ma and appear as tight to isoclinal folds, an intense axial planar foliation, and a N-S-trending stretching lineation parallel to fold axes. Shear sense indicators denote top-N directed shearing. We attribute nappe stacking of the lower Penninic nappes to D1. During this event the Adula nappe was differentially exhumed with respect to nappes presently found in its hangingwall (Tambo-Suretta nappe) and in its footwall (Simano nappe). Thereby it underwent isothermal decompression from eclogite facies conditions of T > 600 °C /P > 20 kbar down to T > 600 °C/ 12 kbar corresponding to an exhumation rate of ca. 7 mm/a.

Structures of the Niemet-Beverin phase (local D2), active between 35 and 30 Ma ago, refold the Adula-Simano nappe boundary. Narrow to tight southwest verging folds at different scales are associated with top-SE directed shearing and are related to exhumation by orogen-oblique stretching. Deformation occurred at P-T conditions of 650–700 °C/ 8–12 kbar during this second stage.

Between 30 and 25 Ma large-scale folds of the Cressim backfolding phase (local D3) refold the gently south dipping D1/D2 foliations into the sub-vertical orientation which is characteristic for the Southern Steep Belt. In the lower Val Mesolcina intense D3 folding is associated with an E-W trending stretching lineation parallel to the fold axes. However, no axial planar foliation developed. During D3 P-T conditions of 650–750 °C/ 4–6 kbar were reached in the southeastern part of the study area. Exhumation during this last stage was mainly the result of rapid erosion, coupled with backfolding and backthrusting along the Insubric mylonites in the Southern Steep Belt.

Exhumation of the Adula nappe was longlasting and occurred between 40 and 25 Ma with an average exhumation rate of 4 mm/a during three distinct major ductile deformation phases. The mechanisms of exhumation differ for each of these stages. Unroofing by gravitational spreading and crustal stretching only plays a subordinate role (D2). Penetrative deformation (D1–D3) progressively concentrated in the south leading to older fabrics preserved further north.

ZUSAMMENFASSUNG

In der südlichen Adula- und Simanodecke sind drei Phasen intensiver Deformation mit Dekompression bei Temperaturen über 600 °C verbunden. Die Zapportphase (lokal D1) vollzog sich zwischen 40 und 35 Ma und führte zur Bildung von engen bis isoklinalen Falten, einer ausgeprägten Achsenebenenfoliation und N-S streichenden Streckungslinearen parallel zur Orientierung der Faltenachsen. Schersinnindikatoren zeigen Top-N gerichtete Bewegungen an, die zur Deckenstapelung führten. Während dieses Ereignisses wurde die Aduladecke bezüglich der Einheiten, die nun im Hangenden (Tambo- und Surettadecke) und im Liegenden (Simanodecke) zu finden sind, differentiell exhumiert. Dabei erfuhr sie eine isotherme Dekompression von eklogitfaziellen Bedingungen von T > 600 °C/ P > 20 kbar bis hinauf zu 600–650°C/ 12 kbar, was einer Exhumationsrate von etwa 7 mm/a entspricht.

Strukturen der Niemet-Beverinphase (lokal D2) entstanden zwischen 35 und 30 Ma und verfalten die bestehende Deckengrenze zwischen Adula- und Simanodecke. Enge südwestvergente Falten unterschiedlicher Grösse sind mit einem Top-SE gerichteten Schersinn assoziiert. Deformation fand bei metamorphen Bedingungen von 650–700 °C / 8–12 kbar statt und wird einer Dehnung schräg zum Orogen zugeschrieben

Zwischen 30 und 25 Ma bildeten sich die Rückfalten der Cressimphase (lokal D3). Sie bringen die mässig einfallenden Strukturen der ersten beiden Phasen in eine subvertikale Orientierung in der Südlichen Steilzone. Im unteren Val Misox ist die Bildung der D3 Falten mit einem E-W streichenden Streckungslinear verbunden, obwohl sich keine neue Achsenebenenfoliation bildete.Während D3 wurden im südlichen Arbeitsgebiet metamorphe Bedingungen von 650 C°/ 4–6 kbar erreicht. In dieser letzten Phase war die Exhumation die Folge von rascher Erosion, die mit Rücküberschiebungen entlang der Insubrischen Mylonite in der Südlichen Steilzone einherging.

Die Exhumation der Aduladecke war ein langanhaltender Prozess und geschah zwischen 40 und 25 Ma während drei Deformationsphasen bei einer Exhumationsrate von durchschnittlich etwa 4 mm/a. Die Prozesse, die zur Exhumation führten, waren für jede Phase verschieden. Gravitativer Kollaps scheint nur eine untergeordnete Rolle gespielt zu haben (D2). Penetrative Deformation konzentrierte sich im Verlauf der Exhumation im Süden, sodass im Norden ältere Strukturen erhalten sind.

[1] Geological Institute at Bonn University, Nussallee 8, D-53115 Bonn, Germany
[2] Department of Earth Sciences, Basel University, Bernoullistr. 30, 4058 Basel, Switzerland
[3] deceased

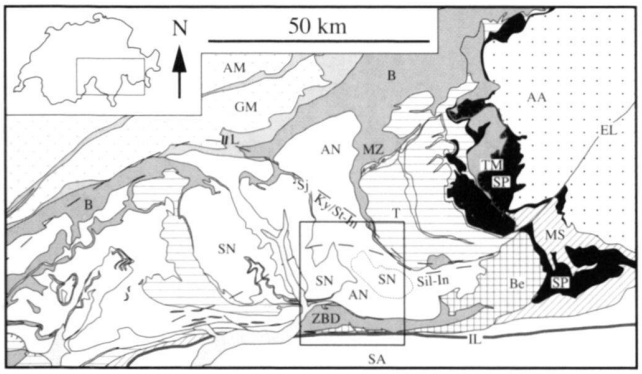

Fig. 1. Tectonic sketch of the Central Alps after Spicher (1980), slightly modified after Froitzheim et al. (1996) and by the authors. The mineral zone boundaries are after Niggli and Niggli (1965). The rectangle indicates the area of investigation. White areas: lower Penninic nappes (European foreland), shaded: N-Penninic Bündnerschiefer and Bellinzona-Dascio Zone; horizontal ruling: Middle Penninic nappes (Briançonnais); oblique ruling: Margna-Sesia nappe; black: Upper Penninic nappes (S-Penninic ocean).
AA: Austroalpine nappes; AN: Adula nappe; AM: Aar massif; B: Bündnerschiefer; EL: Engadin Line; Be: Bergell Intrusion; GM: Gotthard massif; IL: Insubric Line; L: Lukmanier Pass; MS: Margna-Sesia nappe MZ: Misox zone; SA: Southern Alps; SN: Simano nappe; Sj: Soja- syncline; SP: South Penninic nappes; T: Tambo nappe; TM: Turba Mylonite; ZBD: Zone of Bellinzona-Dascio.

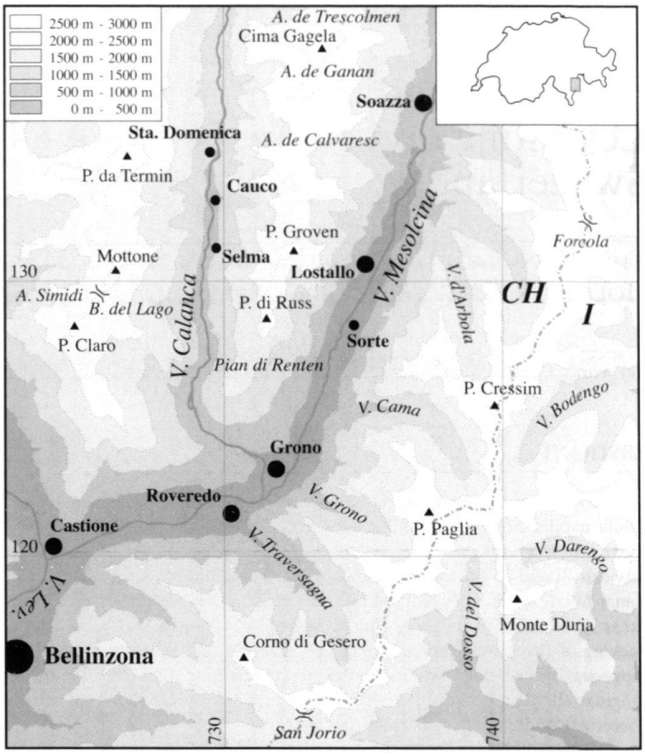

Fig. 2. Topographic reference map of the study area with all localities mentioned in the text. CH: Switzerland; I: Italy; circles: towns /villages; triangles: peaks; Coordinates are from the Swiss national topographic map grid.

Introduction

This work focuses on the deformation and metamorphic history of the Adula and Simano nappes during decompression. These two Lower Penninic nappes (Fig. 1) are well exposed in the southern Moesano (Val Mesolcina and Val Calanca in southern Graubünden/Switzerland; Fig. 2). The early stages of the evolution of these two nappes are very contrasting. The Adula nappe underwent an Alpine eclogite facies metamorphism under P-T conditions of up to 850°C and 30 kbar (Heinrich 1986; Nimis & Trommsdorff 2001). This first metamorphic overprint predates nappe stacking. Relicts of such extreme high pressure are absent in the underlying Simano nappe and all other lower Penninic nappes, as well as in the overlying middle and upper Penninic nappes. The exact age of this high-pressure event in the Adula nappe is still a matter of debate but an Eocene age is indicated by radiometric dating in the laterally adjacent Cima Lunga unit (Gebauer 1996) as well as by structural considerations (Schmid et al. 1996). Subsequent Barrovian type metamorphism of Late Eocene to Oligocene age (e.g. Niggli & Niggli 1965), referred to as „Lepontine metamorphism", postdates nappe stacking. It is one of the aims of this study to unravel the exhumation history of the eclogite facies Adula nappe and the neighboring tectonic units of the Lepontine dome.

On a mesoscopic and microscopic scale we define "deformation phases" primarily on the basis of overprinting relationships. Mapping and correlation of large scale structures within a high grade gneiss complex, however, is more difficult than in lower grade regions where Mesozoic sediments at least partly preserve their original characteristics and may serve as structural marker horizons. Such markers are not available within the complex gneiss series. The existence of dismembered slices of Mesozoic metasediments can only rarely be inferred on purely lithological arguments. Hence, the large-scale geometry of this multiply folded nappe stack can often be deciphered with only limited certainty.

Strain magnitudes associated with the three main deformation phases vary strongly in different parts of the study area. This variation facilitates the establishment of relationships between mineral growth and deformation phases. However, a particular deformation phase may display different P-T conditions from place to place and this should be taken into account when comparing results obtained from different localities. We emphasize that high metamorphic field gradients in P or T may often be artificial in that the equilibration of the metamorphic assemblages may not have occurred simultaneously at different localities (Todd & Engi 1997). We have used metapelites to correlate deformation structures with metamorphism. Firstly, their assemblages are particularly sensitive to P-T changes under amphibolite facies conditions and, secondly, abundant mica provides good control for relating microstructures to particular deformation phases and associated P-T conditions.

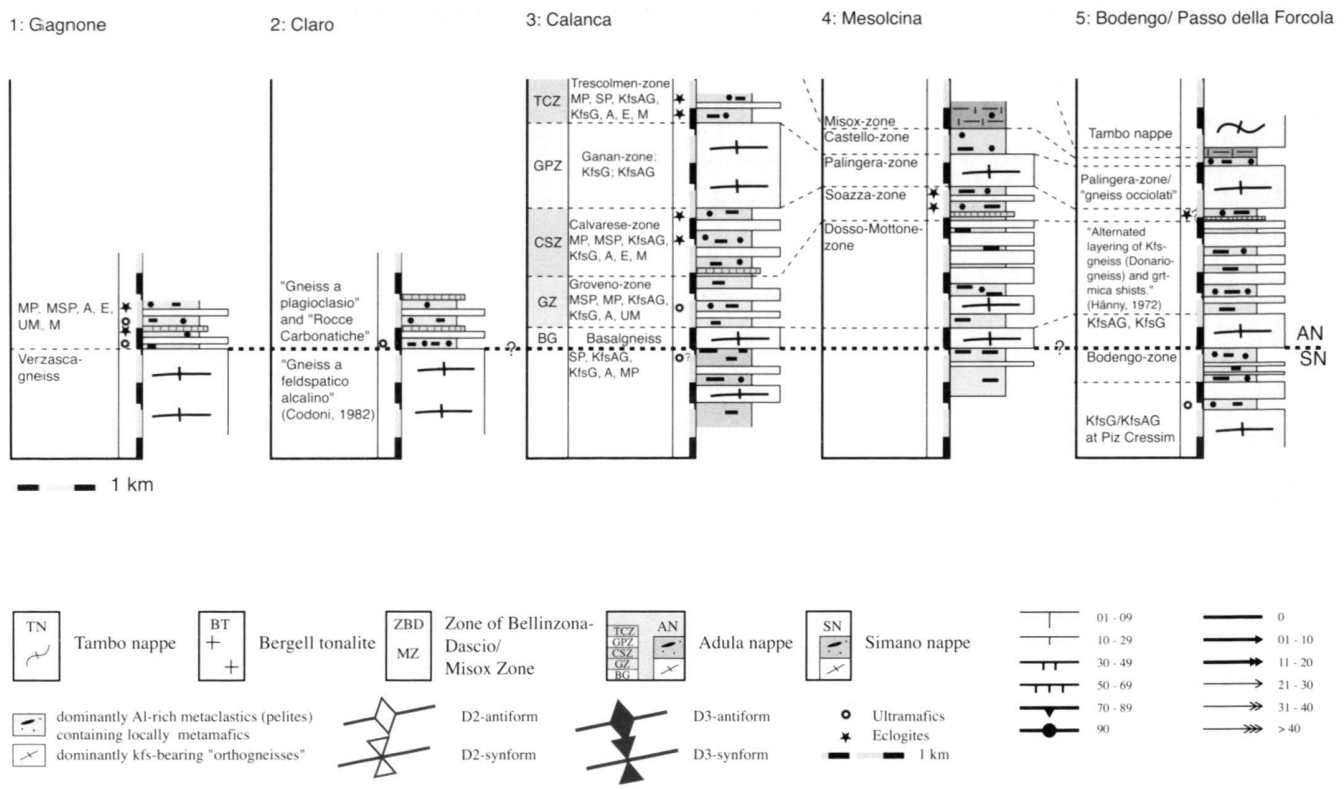

A: amphibolites; E: eclogites; KfsAG: Kfs-augengneiss; KfsG: Kfs-gneiss; M: marbles; MP: metapelites; SP: semipelites
AN, Adula nappe; BA, Borgo antiform; BG, Basalgnaeiss; CA, Cressim antiform; CSZ, Calvarese-Soazza zone;
GPZ, Ganan-Palingera zone; GZ, Groven zone; IL, Insubric line; LA, Leventina antiform; MZ, Misoxer zone;
PA, Paglia antiform; SGA, Sasso della guardia antiform; SN, Simano nappe; ZBD, zone of Bellinzona-Dascio.

Fig. 3. Schematic lithological sequences in 5 areas, four of which (2-5) are located in the study area. Thicknesses are crude estimates. They vary along strike and intense folding may confuse the correlation (see text). (1): Cima di Gagnone (after Grond et al. 1995). (2): Area northeast of Piz Claro (Codoni 1981). (3): Area east of V. Calanca between A. Trescolmen and Selma (Frischknecht 1923; Kündig 1926). (4): V. Mesolcina around Soazza (Weber 1966; Bellin 1929). (5): Area around Passo della Forcola (Hänny 1972; Weber 1966).

Previous work

The earliest workers in the Lepontine Alps (e.g. Studer & Escher 1853) already distinguished three tectonic domains, later defined by Milnes (1974) as Northern Steep Belt, Flat Belt, and Southern Steep Belt. The Northern Steep Belt is situated south of the Gotthard massif and separated from the southern steep belt adjacent to the Insubric Line („root zone") by the flat lying part of the Penninic nappe stack (Milnes 1974). Pioneering work by Rolle (1881) and Heim (1891) led to the interpretation of the Adula gneiss complex as a northwards closing, huge recumbent anticline (a fold nappe or „Deckfalte") by Schardt (1898) and Lugeon (1901). However, Wilckens (1907) and Heydweiler (1918) already showed that the bulk of the Adula nappe does not represent a coherent pre-Alpine gneiss core but rather consists of several thin slices („Teildecken"), separated from each other by sediments of inferred Mesozoic age. Preiswerk (1921) and Kopp (1923a) correlated particular marble horizons found within the Southern Steep Belt with corresponding sedimentary zones, separating individual flat-lying Lepontine nappes further north. From 1923 onwards the Swiss part of the Adula nappe was completely mapped within a short time span, mostly by students of Schardt (Jenny 1923; Kopp 1923b; Frischknecht 1923; Kündig 1926; Strasser 1928; Bellin 1929; Knoblauch et al. 1939). A second period of detailed research took place between 1960 and 1980 under the guidance of A. Gansser and E. Wenk and most of the southern Adula was remapped (Hänny 1972; Bruggmann 1965; Fumasoli 1974; Blattner 1965; Codoni 1982; Weber 1966).

Milnes (1974, 1978) published the first modern structural analysis of the entire Lepontine area and introduced the concept of nappe refolding. He demonstrated that the evolution of the Southern Steep Belt is not genetically related to nappe formation but rather postdates it (Milnes 1974). At the same time petrological investigations focussed on the extremely high

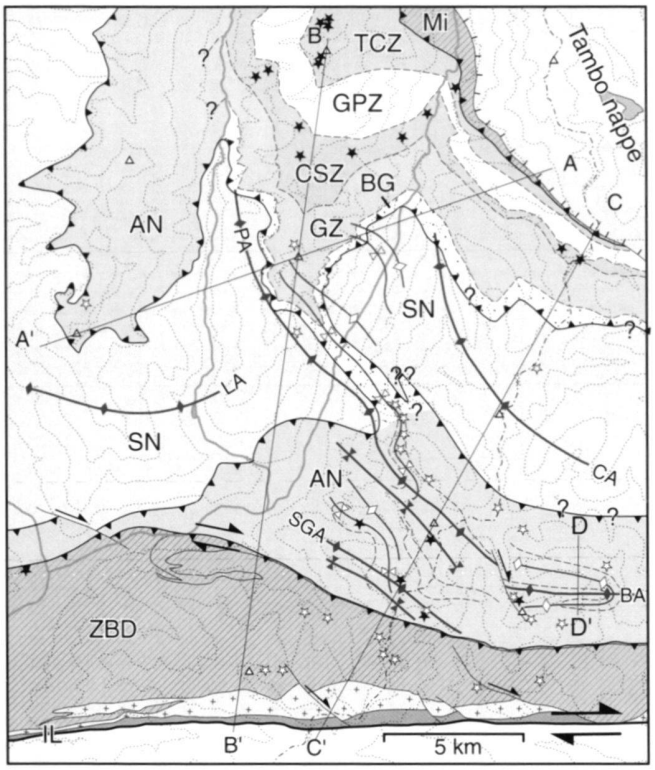

Fig. 4. Structural maps of the study area. The data are compiled from Hänny (1972), Weber (1966), Codoni (1981), Knoblauch et al. (1927), Bruggmann (1965), Kündig (1926), Bellin (1929), Jeker (2000), Niederberger (2000), Frischbutter (2000), Damo (2000) and this investigation. Legend is the same as for Fig. 3.

Fig. 4a. Schematic tectonic map of the study area. Positions of cross sections (Fig. 5a–5c) and traces of axial planes for large-scale D2 folds (thin lines) and D3 folds (thick lines) are indicated. Black stars denote occurrences of eclogites, white ones occurrences of ultramafics.

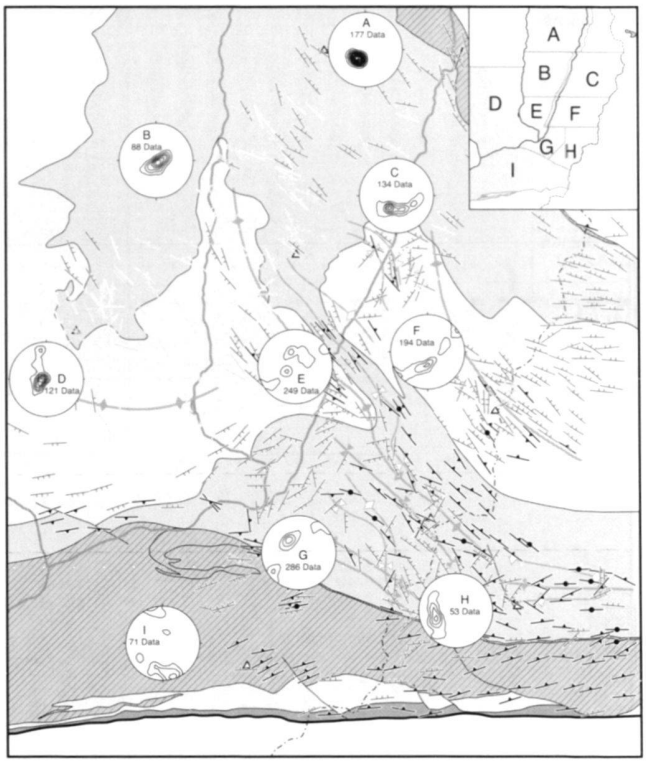

Fig. 4b. Map of main foliation (S1,2 or 3). Stereoplots A-I (subareas given by inset): poles to foliation, interval between contour lines is 2.5.

metamorphic field gradient observed in our study area (e.g. Niggli & Niggli 1965) and on the possibility to study isograds in three dimensions (Klein 1976; Thompson 1976). Van der Plas (1959), Heinrich (1986) and Löw (1987) showed that the Adula nappe underwent regional high-pressure conditions during the Alpine orogenic cycle. Finally, several workers started to combine structural and petrological methods in order to unravel the complex history of the Adula nappe (Löw 1987; Plas 1992; Huber 1993; Grond et al. 1995; Partzsch 1998).

The nappe edifice within the working area

General remarks and regional setting

The lower Penninic Simano and Adula nappes constitute most of the study area (Fig. 3, Fig. 4). They are attributed to the distal European continental margin and were subducted towards the south, beneath the Apulian microplate and previously accreted middle and upper Penninic units during the late Eocene (Schmid et al. 1996). The Adula nappe does not represent a coherent thrust unit or nappe like most of the other Penninic basement nappes. It consists of lithologically heterogeneous and intensely deformed imbricates. However, we collectively refer to these imbricates as the Adula nappe. The imbricates are made up of numerous thin slices of Variscan metagranitoids, paragneisses, scarce occurrences of mafics and ultramafics, and probably Mesozoic metasediments. Lenses of partly preserved mafic eclogites are commonly embedded within metapelites of unknown but probably Mesozoic age. In contrast, the Simano nappe is a relatively coherent thrust sheet and predominantly consists of thick pre-Mesozoic metagranitoids. In its upper part pre-Mesozoic metaclastics and amphibolites are frequent (Jenny et al. 1923). In their frontal parts the Adula and Simano nappes are separated by the Mesozoic cover of the Simano nappe, referred to as the „Soja syncline" (Fig. 1). Towards the south these sediments wedge out and the nappe boundary becomes ambiguous.

Towards the northeast the Adula nappe is overlain by the Misox zone, which is also a zone of imbricates (Fig. 1, Fig. 4). These imbricates largely consist of clastic marine sediments

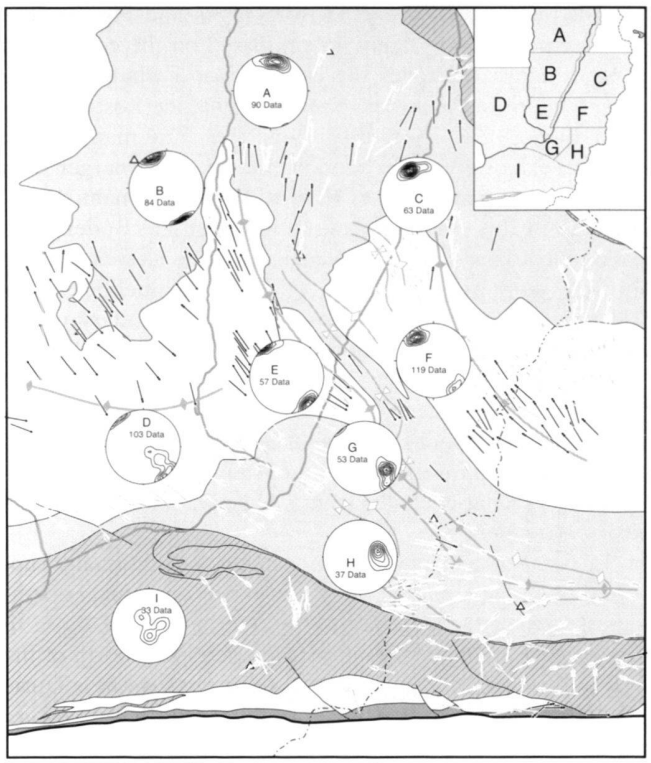

Fig. 4c: Map of main stretching lineations (L1,2 or 3). Stereoplots A-I (subareas given by inset) lineations, interval between contour lines is 2.5.

(Bündnerschiefer) deposited in the North Penninic (or Valais) basin located south of the European margin (Steinmann & Stille 1999). Also gneissic slices indistinguishable from those in the Adula nappe occur (Partzsch 1998). Schmid et al. (1996) also attribute the lithologically heterogeneous Zone of Bellinzona-Dascio, juxtaposed with the Adula nappe in the southern part of the working area, to the North Penninic basin (Fig. 1, Fig. 4a). Towards the southeast, the Misox zone is cut off by the Miocene Forcola normal fault (Meyre et al. 1999a) and the Adula nappe is directly juxtaposed to the next higher nappe, the middle Penninic Tambo nappe, which is regarded as a part of the Briançonnais microcontinent (Schreurs 1993; Schmid et al. 1996; Baudin et al. 1993).

Regional high-pressure metamorphism of the Adula nappe is attributed to Paleocene to Eocene subduction (Froitzheim et al. 1996). From north to south peak P-T conditions related to this high-pressure stage progressively increase from blueschist facies conditions (12 kbar, 500 °C) in the north to eclogite facies conditions (800 °C/ >30 kbar) in the south (Van der Plas 1959; Heinrich 1986; Löw 1987; Meyre et al. 1997; Nimis & Trommsdorff 2001). This high-pressure metamorphism is not documented in the Simano nappe while the Tambo nappe records more moderate peak pressures around 12 kbar (Baudin et al. 1993).

Lithological successions within the Adula nappe and mapping of nappe boundaries in the study area

The Adula nappe predominantly consists of pre-Mesozoic metagranitoids and Aluminium-poor metaclastics. These dominating lithologies are locally interlayered with metapelites, partly eclogitic amphibolites and scarce ultramafics whose protolith ages are unknown, as well as with Mesozoic quartzites and marbles. In the following we will discuss these lithological sequences in conjunction with the question of the position of the nappe boundary between the Adula and the Simano nappe south of the Soja syncline (Fig. 3 & Fig. 4).

The prominent and up to 15 m thick marble horizon exposed at the top of Pizzo Claro is generally accepted to represent the nappe boundary with the underlying Simano nappe (e.g. Spicher 1980). We have some objections to this view. These marbles are embedded within a strongly foliated sequence of paragneisses and layers of Kfs-augengneisses and all units are intensely folded together during our second deformation phase D2 (see Strasser 1928; Codoni 1982). Amphibolites are frequent and up to 30 meters thick lenses of ultramafics (e.g. above Alpe Simidi) may also be found in this sequence which overlies a several hundreds of meters thick unit dominated by less intensely foliated Kfs-"orthogneisses" (Codoni 1982). Several additional layers of marble, often associated with calcsilicates, are present above and below this prominent marble (Kopp 1922; Codoni 1982). Jenny et al. (1923) and Strasser (1928) traced the sediments of the Soja syncline into another marble horizon found in a higher structural position at Piz Termin (see Staub 1930; Heinrich 1986). Additionally, marbles are commonly found further away from the suspected nappe contact within the strongly sliced Adula nappe, so that the significance of the marble at Pizzo Claro as a marker between the Adula und Simano nappe is highly questionable. As depicted in Fig. 3, the sequence in the Claro area resembles very much that found at Cima di Gagnone, west of the study area, where various gneisses, containing ultramafics and marbles, lie on top of a monotonous Kfs-gneiss, the so called „Verzasca-Gneiss" (Grond et al. 1995). Ultramafic bodies and eclogites found immediately above the top of the Verzasca-Gneiss display high pressure assemblages typical for the Adula-nappe (e.g. Heinrich 1986). Hence, at Cima di Gagnone the nappe boundary is generally defined at the top of the Verzasca-Gneiss (Grond et al. 1995). In analogy we set the nappe boundary at Pizzo Claro in a deeper position than the predominant marble horizon and immediately above the less intensely foliated Kfs-"orthogneisses" of Codoni (1982). However, no relicts of high pressure have yet been found in the overlying strongly foliated base of the Adula nappe in the Claro area.

Based on lithological differences the succession found east of Val Calanca are grouped into five subunits (Fig. 4a) and correlated in Fig. 3. The „Groven-zone" (GZ; „Grovenonappes" in the sense of Kündig, 1926) and the „Calvarese-Soazza zone" (CSZ) (Frischknecht 1923; Weber 1966; Hänny

1972) display similarities to the miscellaneous gneisses at the base of the Adula nappe at Pizzo Claro. The strongly heterogeneous CSZ consists of metapelites which contain lenses of partly eclogitic amphibolites, semipelites and augengneisses, and also includes marbles at its base which reach a thickness of 20 m at Passo Calvarese. The Groven zone (GZ) dominantly consists of well foliated augengneisses and garnet-plagioclase-mica schists (semipelites), locally interlayered with banded amphibolites. It also contains an ultramafic body, 300 m in size, at Piz Groven. This GZ is less abundant in Al-rich pelites and no marbles or eclogites have been found yet.

East of Val Calanca a 200–300 meters thick band of pale, massive two mica orthogneiss, partly developed as augengneiss („Basalgneiss", Kündig 1926; Rüti 2001) represents the base of the Adula nappe (Fig. 3) and is locally underlain by amphibolites and calcsilicates (e.g. at the top of Pizz di Rüss) which mark the nappe boundary between the Simano and the Adula nappe. However, this Basalgneiss cannot be traced westwards cross Val Calanca and is absent at Pizzo Claro. Conversely, the thick „orthogneisses" which define the top of the Simano nappe west of Val Calanca cannot be traced eastward across this valley. The nappe boundary is strongly folded by D2 folds in many places and no original structure such as a distinct mylonite horizon, as found at the base of the Adula nappe further in the north (Partzsch 1998), is present in our study area. It is possible that the complications described above originate from isoclinal large scale folding of the base of the Adula nappe during D2 in Val Calanca.

However, the Basalgneis is a valuable marker horizon east of Val Calanca. There, Frischbutter (2000) was able to trace the Simano-Adula nappe boundary into the eastern flank of Val Mesolcina and back westwards into marble layers which define the base of the Adula nappe in the lowermost Val Calanca (see Fig. 4a). A major D3 antiform, the Paglia-antiform, is responsible for this large scale excursion of the nappe contact. The marble horizon in the lowermost Val Calanca is already part of the Southern Steep Belt (see Fig. 4a) and corresponds to the so-called „Algaletta-marble", defined in the Val Leventina section (Codoni 1982; Staub 1916; Kopp 1922; Strasser 1928).

Across Val Leventina the Adula (= Cima Lunga) nappe becomes extremely thin. The Algaletta and the Castiones marble define the upper and lower boundary of the Adula nappe, respectively (e.g. Kopp 1922). Eastwards the Castione-marble which defines the top of the Adula nappe remains in a steep orientation and continues straight into the „Paina-marble" found east of Val Mesolcina. The Paina marble was mylonitized under greenschist facies conditions and marks a late dextral strike slip fault (Fumasoli 1974; Heitzmann 1974, 1975, 1987) defining the southern boundary of the Adula nappe against the Zone of Bellinzona-Dascio (Fig. 4a) all the way to Valle della Mera (Fumasoli 1974; Heitzmann 1974).

The subunits forming the flat lying part of the Adula nappe between Val Calanca and Val Mesolcina in the northern part of the study area can be followed with some certainty further towards the east (northern part of Fig. 4a and Fig. 3). The mapping proposed in figure 4a and based on the correlation given in figure 3, implies the existence of a window of the Simano nappe in the middle Val Mesolcina, the Lostallo window (Kündig 1926). According to our structural mapping the eastward extension of this window must be much larger than proposed in previous studies (Bellin 1929; Bruggmann 1965). The core of this window, exposed in upper Val Bodengo, is made up by thick, massive Kfs-gneisses while its western and northern margins dominantly consist of semipelitic schists (Hänny 1972). However, the southwestern boundary of the window remains highly ambiguous. The lower Basalgneiss, which still defines the base of the Adula nappe west of Val Mesolcina, can be traced eastwards into monotonous gneisses in Val Cama and gradually looses its characteristics in terms of a marker horizon for the base of the Adula nappe. The Lostallo-window primarily results from a huge D2 antiform, as will be discussed later.

The existence of the Lostallo window is additionally supported by the distribution of high-pressure assemblages. Retrogressed eclogites (Fig. 4a) are present in the CSZ close to Passo della Forcola (Weber 1966; Heinrich 1986) north of the supposed window and again south of this window at Piz Duria (e.g. Heinrich 1986). Additional localities with high-pressure assemblages have been documented in our study (Fig. 4a). Garnet-amphibole-symplectites in Val Grono, first described by Bruggmann (1965), turned out to contain fresh domains showing the eclogite facies assemblage Omp + Grt + Rt.

The structural buildup

Rocks in the study area, particularly in the Adula nappe, experienced extreme deformation and commonly display a well developed foliation and stretching lineation. Intense and repeated folding developed almost exclusively under amphibolite facies conditions. We found three major ductile deformation phases in our working area which may correspond to those first described by Ayrton & Ramsay (1974).

1. The first deformation phase D1 is associated with isoclinal folding and the formation of the main foliation S1 and a stretching lineation L1 in most parts of the study area. During this phase the Adula nappe was thrusted towards north onto the Simano nappe. Simultaneously, substantial exhumation from eclogite to amphibolite facies condition occurred in the Adula nappe.
2. During the second deformation phase D2 the established nappe pile was affected by tight southwest-verging folds at different scales. This deformation intensifies towards the south where a new streching lineation L2 and a new axial planar foliation S2 developed. Top-SE shearing parallel to the orientation of fold axes accompanied D2. We propose that the Southern Steep Belt was active as a south dipping ductile shear zone with a normal sense offset during this stage of deformation.

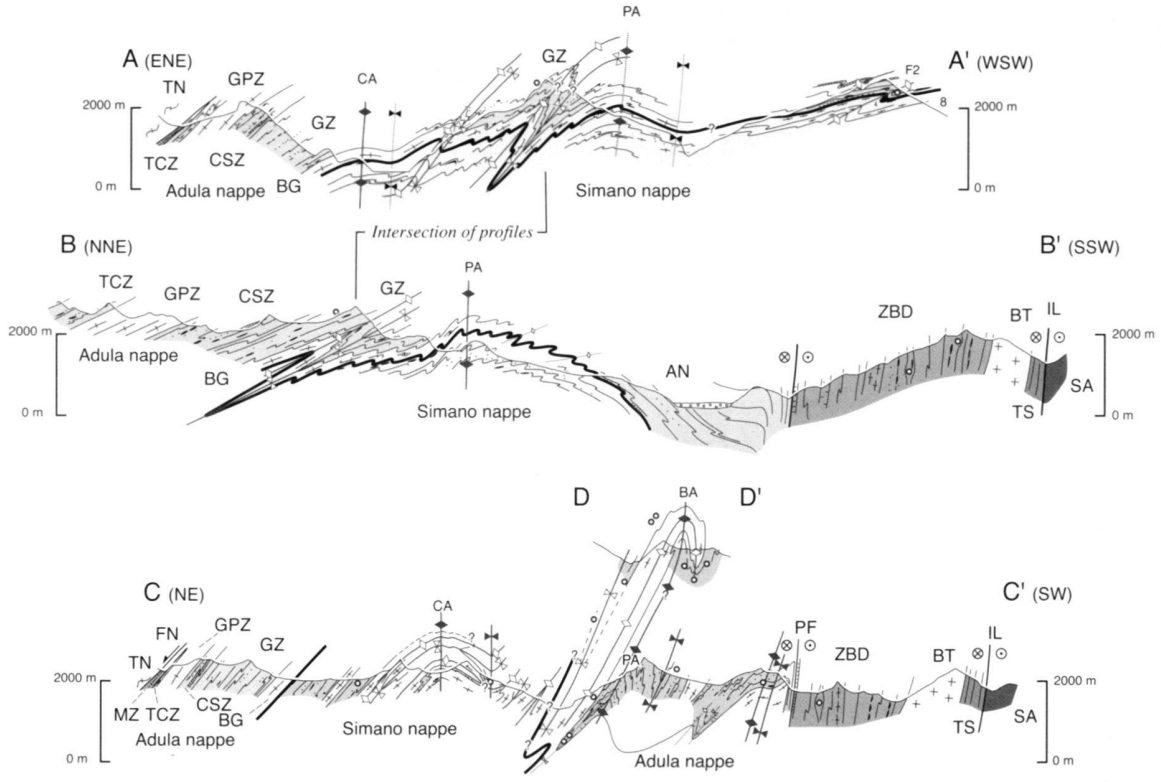

Fig. 5. Schematic cross sections through study area. The positions of cross sections (A-A', B-B',C-C', D-D') are indicated in Fig. 4a. Legend is the same as for Fig. 3.

3. Folds of the third deformation phase D3 relate the flat belt in the north with the Steep Belt in the south. In the southeastern study area, where tight D3 folds are formed, a new streching lineation L3 is observed. The so called "Paglia-Schlingenkomplex" (Bruggmann 1965) results from D2-D3 interference of large scale folds.

At first sight it may appear odd to present foliation and lineation maps (Figs. 4b and 4c) in an area which underwent multiple deformation without attributing the displayed structural elements to particular deformation phases. However, rocks exhibiting more than one foliation can only be found in fold hinges of D2 folds and, generally, no foliation is associated with D3 folding. Rocks with more than one lineation are virtually absent in the study area and it turned out that all fold axes and/or stretching lineations of the three deformation phases (D1 to D3) are commonly coaxial. Fold interference patterns are of type 3 (Ramsay & Huber 1987). Hence, the lineation map simultaneously illustrates the orientation of all stretching lineations and fold axes (Wenk 1955) formed during D1 to D3. The stereoplots in figures 4b and 4c illustrate that foliations generally define great circles with an axis subparallel to the main stretching lineation (L1 or L2) in any given area. L1 and L2 are generally associated with a considerable stretch parallel to the D1 or D2 fold axes. We suppose that this linear anisotropy forced D3 fold axes to form in a sub-parallel orientation (Cobbold & Watkinson 1981).

The foliation map (Fig. 4b) map displays the main foliation, commonly subparallel to layering, and the composite D1-D2 foliation. The gentle dips towards northeast in the northern part are reoriented into steep to overturned positions characteristic for the Southern Steep Belt by backfolds whose fold axes closely follow the pre-existing trend of the D1-D2 lineations (compare with Fig. 4c). East of Val Mesolcina a series of large scale backfolds of the third generation (D3), rather than a single backfold, are seen to affect the foliations – and hence the entire nappe pile – north of the Paina marble (see Cressim- Paglia- and Guardia-antiforms depicted in the cross sections of Fig. 5). At least one of these antiforms seems to be cut by the post-D3 Paina marble strike slip fault (see southern end of profile C-C' in Fig. 5). West of Val Mesolcina, however, one single antiform, whose axial trace dies out eastward, connects the flat lying nappes to the Southern Steep Belt.

All lineations shown in the map of Fig. 4c are defined by elongated mineral aggregates (e.g. qtz or pl) or aligned acicular minerals (e.g. am), while the fold axes which follow the same trend are not included. The strike of the lineations progressively rotates from N-S over NW-SE to E-W. The NW

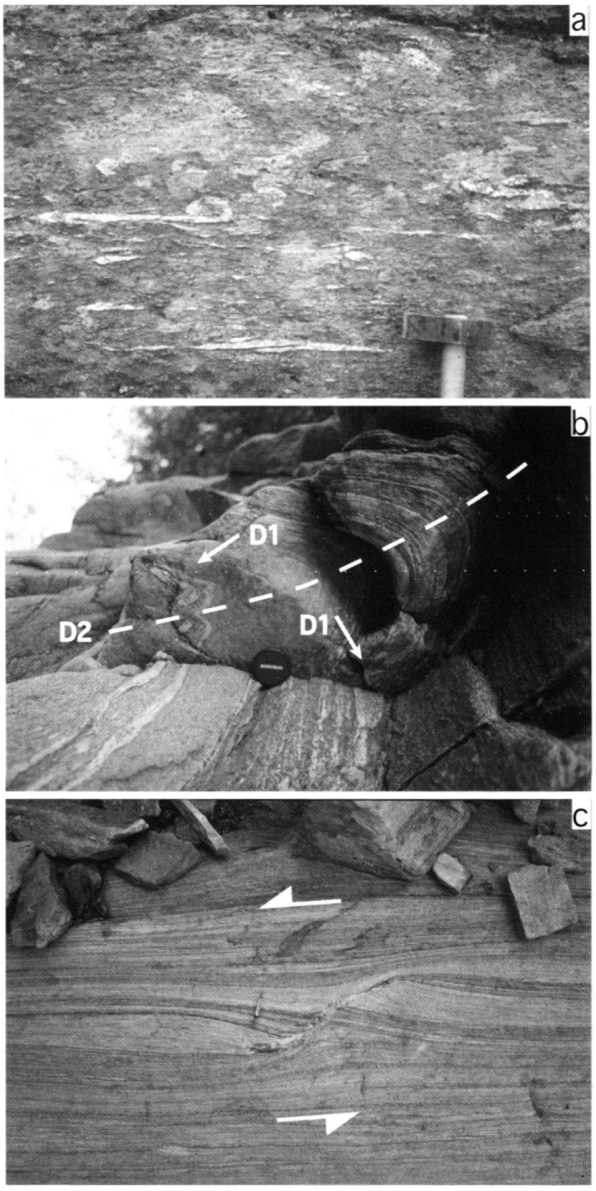

Fig. 6. Photographs illustrating D1 structures:
(a) Isoclinal dismembered D1 folds in metapelites (Alp Calvaresc/ Calanca), refolding a pre-D1 foliation.
(b) Isoclinal D1 folds, refolded by a tight D2 fold. Lower Auriglia-gorge (Selma, Calanca).
(c) Shear band and associated oblique boudinage in Kfs-gneisses indicating a sinistral shear sense (= top N; Pass de Ganan, Calanca).

plunge changes into a SE plunge along a culmination situated a few kilometers north of the Southern Steep Belt. This general feature of progressive anticlockwise rotation of the predominant stretching lineations is typical for the entire southern part of the Lepontine dome (Wenk 1955). Note, however, that these predominant lineations are not attributed to one single deformation phase.

We now describe the macro- and mesoscopic aspects of the three major deformation phases D1 to D3 in more detail. Microstructures and precise P-T conditions related to these penetrative ductile structures will be discussed later. In this work we concentrate on the amphibolite grade deformation history of the Simano and Adula nappes. The D1 of this study postdates earlier high pressure deformation phases such as the Sorreda phase of Löw (1987) and/or the Trescolmen phase of Partzsch (1998) and Meyre et al. (1997). Post-D3 deformation, e.g. dextral strike slip along the Paina marble and related faults, took place at considerably lower grade metamorphic conditions.

Pre-D1 and D1 structures

In a purely structural sense the D1 structures correspond to the Zapport phase of Löw (1987). They are best preserved in the northern part of the study area (Alp de Trescolmen, Alp de Ganan) where the S1 schistosity is not strongly overprinted by subsequent deformation as is the case further south. In this northern area, the dominant foliation is related to isoclinal, D1, similar folds (Fig. 6a,b). The stretching lineation typically dips N to NNE and is consistently oriented parallel to the N-S striking D1 fold axes. Dismembered folds (Fig. 6a) indicate intense deformation during D1 and no large scale D1 folds have been found. Abundant shear sense indicators (shear bands, σ-clasts, asymmetric boudins) on a mesoscopic and microscopic scale indicate top-to N shearing (Fig. 6c), related to nappe stacking during D1. The L1 stretching lineation is defined by elongated quartz and feldspar aggregates, amphiboles and strings of boudinaged competent material. In metasediments and amphibolites found in the northern part of the study area all minerals with a platy and acicular shape are commonly aligned parallel to the S1-foliation and even within D1 fold hinges no pre-D1 minerals are discernible. Only metaclastics occasionally contain white micas forming discordant microlithons predating S1.

Bending of the S1 foliation around eclogitic boudins documents that S1 postdates high-pressure conditions in the Adula nappe (Partzsch 1998). Along their rims such boudins are commonly retrogressed to garnet-bearing amphibolites during D1 (Heinrich 1986). Garnet-omphacite-bearing assemblages within eclogitic boudins sometimes define an older planar fabric (pre-D1 Trescolmen-phase of Partzsch 1998), completely dismembered from D1 and only found in isolated boudins. In conclusion, D1 is related to nappe stacking in the lower Lepontine area and postdates an earlier eclogitic event in the Adula nappe. The subsequent phases (D2 and D3) described below overprint the nappe boundaries established during D1 (see also Ayrton & Ramsay 1974; Grujic & Mancktelow 1996).

D2 structures

Structures of this phase are dominant in the central part of the study area where subsequent D3 overprint is weak. This sec-

ond phase refolds the Simano-Adula nappe boundary on a large scale. In particular, we confirm the existence of a window of the Simano nappe around Lostallo proposed by Kündig (1926). The window results from an antiform formed during D2. The northern limb of this antiform is affected by a series of southwest-verging large scale folds (Kündig 1926). One of them is exposed right at Lostallo (see Fig. 4), where it causes a subvertical to overturned (= steeply NE-dipping) orientation of the D1 foliation on the eastern side of Val Mesolcina (Fig. 4 & Fig. 5a). Further south, at Sorte in Val Mesolcina, foliations display subvertical dip over an approximately 3 kilometres wide zone (Fig. 4b). This steep zone, situated several kilometers north of the Southern Steep Belt, is interpreted as the southern limb of the huge D2 antiform forming the Lostallo window and an adjacent isoclinal synform south of it. The Adula nappe is folded down and below the valley floor in the core of this tight D2 synform. This leads to the separation of the Lostallo-window from the rest of the Simano nappe (Fig. 4a). The so called „Paglia-Schlingenkomplex" (Bruggmann 1965) in the southeastern part of the study area is formed by a superposition of D2 and D3 folds. The „Duria-synform" (Fumasoli 1974) also represents a large scale D2 fold, folded around a D3 antiform („Borgo antiform"), representing the eastward continuation of the D3 „Paglia-antiform" (Fig. 4a; Fig. 5c). Hence, the „Duria-synform" in fact represents a former D2 antiform exposed on the southern limb of a D3 antiform.

D2 fold style strongly varies on a mesoscopic scale, from more open to tight isoclinal folds, as a result of lithological heterogeneities. In the Adula nappe D2 is not the main folding phase in contrast to other parts of the Lepontine area (Ayrton & Ramsay 1974; Milnes 1978; Grujic & Manckelow 1996). While a new axial planar foliation S2 clearly is present in the hinges of open to narrow D2 folds, S1 is rotated into an orientation parallel to S2 in the limbs and the overall schistosity is considered to be the result of D1 and D2 deformation.

North of the Southern Steep Belt D2 folds are consistently southwest-vergent (Fig. 6b, 7b). The S2 axial plane foliation is mainly defined by synkinematic biotite in leucocratic gneisses. Even relatively open D2 folds often display a pronounced stretching lineation L2, suggesting that D2 fold axes initially developed parallel to the stretching lineation (see Stünitz 1991). L2 is easily distinguished from L1 since shear sense indicators related to L2 consistently show top-SE directed movement (Fig. 7c). Since SE-directed shear sense indicators are clearly present on both limbs of D2 folds, this folding is interpreted to be coeval with top to SE shearing. Within metapelites these shear-indicators are clearly associated with the S2-foliation and its characteristic mineral assemblages.

Interestingly, the locus of the onset of strong D2 deformation coincides with that of the anticlockwise rotation of the dominant stretching lineation from N-S to NW- SE. Because the stretching lineations trend NW-SE (Fig. 4c) in the central part of the working area where D2 is best developed, we propose that this bending of the lineations results from D2. We conclude that top-N and N-S oriented L1 stretching lineations become progressively overprinted by top-SW and NW-SE trending L2 lineations.

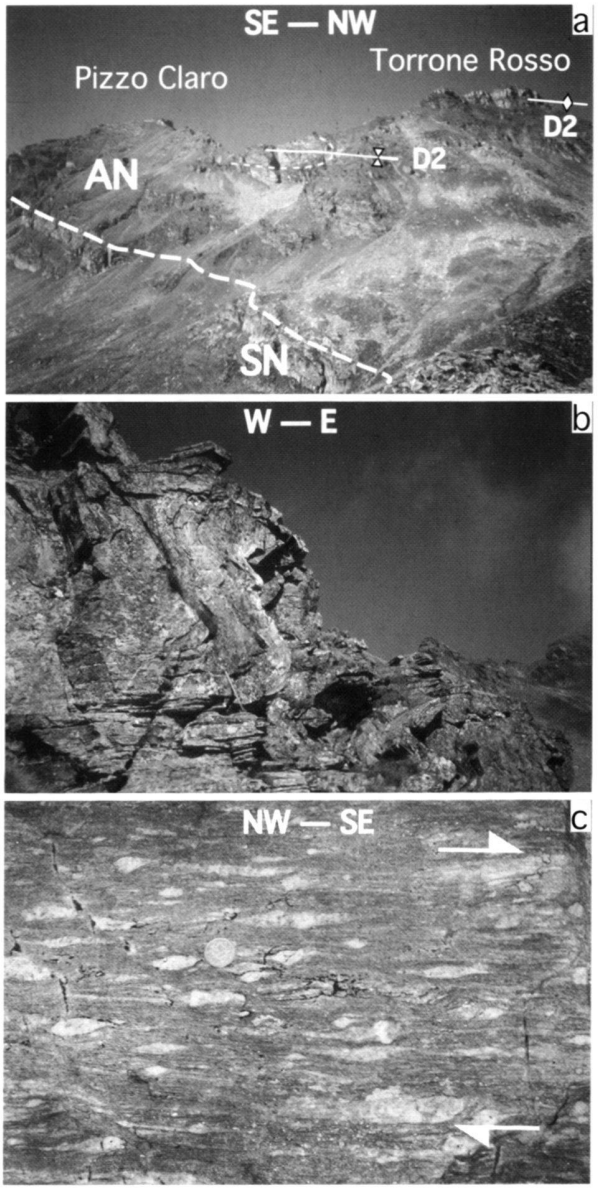

Fig. 7. Photographs illustrating D2 structures:
(a) View towards SW in the Claro area: At Torrone Rosso the marble exposed at the top of Pizzo Claro is doubled due to D2 folding by the tight D2 northward closing synform north of Pizzo Claro (axial plane indicated) already mentioned by Kopp (1922).
(b) Typical SW-verging, narrow D2 fold in a semipelitic gneiss (Borcetta del Lago, Calanca; view towards north; note hammer for scale). Such folds display a distinct axial plane foliation and a pronounced stretching lineation parallel to the fold axis, associated with top-SE directed shearing.
(c) σ-clasts in Kfs-augengneiss indicating dextral shearing during formation of the S2 schistosity S2 (= top-SE; Mottone, Calanca).

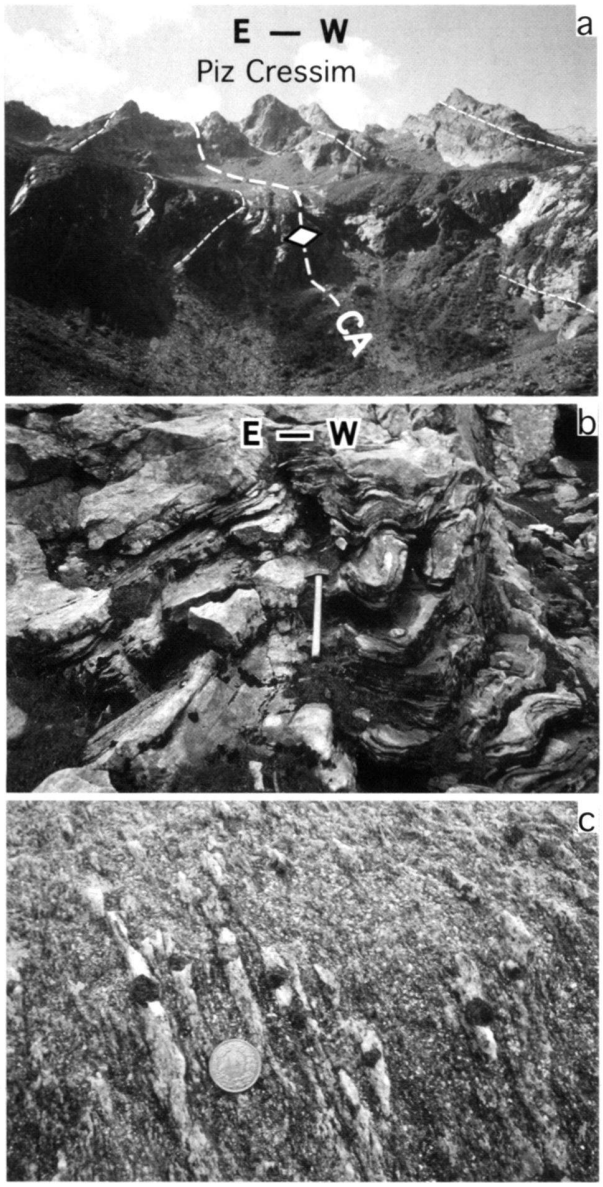

Fig 8. Photographs illustrating D3 structures:
(a) Large scale, open D3 antiform at Piz Cressim (upper Val d' Arbola, Mesolcina; view to the south). Cressim antiform and traces of pre-D3 foliation (thin dashed lines) are indicated.
(b) Open D3 small scale folds (Val d' Arbola, Mesolcina).
(c) Sil-Qtz rods („Faserkiesel") in pressure shadows of garnets defining D3 streching lineation in metapelites. D3 small scale folding is tight, parallel to L3 and synmigmatic in this area (upper Val Grono, Val Mesolcina).

D3 structures

In the southeastern part of the study area D3 folds strike E-W and form tight folds in the „Paglia-Schlingenkomplex" (Bruggmann 1965). Towards north they gradually change their orientation towards a NW-SE and, finally, a N-S oriented strike (Fig. 4). This rotation of the fold axes is associated with a reduction in strain intensity: D3 folds at all scales become progressively more open and cease to exist northwards.

The Cressim-antiform is the most famous of these D3 folds (Kopp 1923b) and we propose the term Cressim phase for this stage of deformation. At Piz Cressim this fold is rather open (Fig. 8a), the fold axis dips to the NW and the axial plane is vertical. In the lower Val d'Arbola the antiform is hardly visible any more and ceases to exist across the Val Mesolcina. Conversely, the antiform tightens towards southeast in Italy and the axial plane progressively rotates from a NW-SE strike into a W-E strike (Hänny 1972; Blattner 1965; Heitzmann 1974; Berger et al. 1996). The Paglia-antiform situated further west (Kopp 1923b; Bruggmann 1965) exhibits exactly the same characteristics and can be traced over a distance of 25 km through the study area. West of Val Calanca one large scale E-W-striking backfold, referred to as „Leventina Antiform", relates the flat belt in the north to the steep belt in the south (Codoni 1982; Fig. 4). The Leventina backfold displays considerable geometric differences to and is disconnected from the other D3 folds situated further east. In spite of this disharmony we regard all of the above described folds to have formed contemporaneously during D3 because they all represent backfolds which reorient the gentle dips in the north to the Southern Steep Belt. East of the working area D3 folding is synmagmatic with the Bergell intrusion and folds its base (Davidson et al. 1996). Since the Bergell batholith intrudes a preexisting steep zone, Berger et al. (1996) argued that the formation of parts of the Southern Steep Belt predates the Bergell intrusion and hence the above mentioned D3 folds. This indicates that the steepening of the southern parts of the Southern Steep Belt, in particular the Tonale series adjacent to the Insubric line, pre-dates D3 folding (compare with the pre-32 Ma old „2. backfolding phase" of Spillmann 1993).

While D3 folds do not show a pronounced axial plane foliation they exhibit a distinct lineation parallel to F3 within the Paglia-Schlingenkomplex. This lineation is defined by synkinematic biotite flakes, quartz fibers and quartz-sillimanite rods (so called „Faserkiesel"). It has been interpreted as a crenulation or intersection lineation by previous authors (Huber 1993; Grond et al. 1995). However, quartz-sillimanite rods, clearly postdating D2, form elongated pressure shadows parallel to D3 fold axes in metapelites (Fig. 8c), indicating a considerable stretch parallel to D3 fold axes associated with constrictional strain in the southeastern part of the study area (see also Steck 1999). Granitoid rocks experienced migmatisation during D3 folding, as documented by melt pockets oriented parallel to D3 axial planes (Huber 1993).

In the central part of the study area the open D3 fold axes occasionally display a small but discernable angle with the dominant lineation. This indicates that D3 refolds L1 and/or L2, even though the D3 fold axes are commonly coaxial with L1 and/or L2 . At Piz Cressim, for example, dominant folding visible on the outcrop scale is related to D2 while these D2 axial planes are bent around the large scale D3 Cressim antiform which formed coaxially with F2 (Damo 2000). Hence,

Table 1. Representative chemical analyses of the samples TN212, TN349, and TN236.

	TN212 Bulk	Phe core	Phe rim	Phe contact ky	Phe contact bt	Grt 2nd Ca-shell	Grt rim	Grt 1st Ca-shell	Grt core	Bt	Bt	Pl	Pl	St
SiO2	59,39	51,97	51,31	49,79	47,14	37,66	38,16	38,17	38,64	36,09	37,37	61,7	62,14	28,54
TiO2	0,79	0,11	0,16	0,45	0,53	0,00	0,00	0,00	0,00	1,27	1,5	0,08	0,05	0,25
Al2O3	20,27	27,22	28,63	28,97	32,50	20,74	20,34	20,31	19,99	17,34	17,65	23,13	24,01	53,06
FeO	5,18	2,01	1,90	1,62	1,27	32,44	32,81	31,35	32,07	17,63	16,31	0,21	0,23	11,02
MnO	0,20	0,00	0,10	0,00	0,03	2,07	1,85	1,46	1,53	0,14	0,08	–	–	0,23
MgO	1,75	3,16	2,61	2,45	1,20	4,43	5,03	4,95	5,76	12,83	12,61	0,00	0,01	2,03
CaO	0,59	0,00	0,00	0,00	0,00	3,54	1,95	3,80	2,01	0	0,04	4,96	5,33	0,00
Na2O	0,80	0,43	0,72	0,83	1,23	0,02	0,04	0,01	0,05	0,3	0,33	9,04	8,78	0,00
K2O	4,93	11,09	10,20	10,23	9,96		0,00	0,02	0,00	9,15	9,07	0,09	0,03	0,00
ZnO														2,78
Sum	93,90	95,99	95,63	94,34	93,86	100,90	100,18	100,07	100,05	94,75	94,96	99,21	100,58	97,91
Si	60,18	6,88	6,79	6,69	6,36	5,97	6,07	6,06	6,12	5,48	5,60	2,76	2,74	8,01
Ti	–	0,01	0,02	0,05	0,05	0,00	0,00	0,00	0,00	0,15	0,17	0,00	0,00	0,05
Al	24,21	4,25	4,47	4,59	5,17	3,88	3,81	3,80	3,73	3,10	3,12	1,22	1,25	17,54
Fe	4,40	0,22	0,21	0,18	0,14	4,30	4,36	4,16	4,25	2,24	2,04	0,01	0,01	2,59
Mn	–	0,00	0,01	0,00	0,00	0,28	0,25	0,20	0,21	0,02	0,01	0,00	0,00	0,05
Mg	2,64	0,62	0,51	0,49	0,24	1,05	1,19	1,17	1,36	2,90	2,82	0,00	0,00	0,85
Ca	0,65	0,00	0,00	0,00	0,00	0,60	0,33	0,65	0,34	0,00	0,01	0,24	0,25	0,00
Na	1,57	0,11	0,18	0,22	0,32	0,01	0,01	0,00	0,02	0,09	0,10	0,78	0,75	0,00
K	6,37	1,87	1,72	1,75	1,72	0,00	0,00	0,00	0,00	1,77	1,73	0,01	0,00	
O	168,34	22,00	22,00	22,00	22,00	24,00	24,00	24,00	24,00	22,00	22,00	8,00	8,00	46,50
Sum cations	100,00	13,97	13,91	13,96	14,01	16,02	16,03	16,04	16,02	15,75	15,59	5,02	5,01	29,67

	TN349 Bulk	Phe	Bt	Grt core	Grt rim	Grt grain b.	Pl contact garnet	TN236 Bulk	Large Grt core	large grt rim	small Grt	Phe	Bt	Pl rim
SiO2	59,22	46,93	34,54	37,89	37,49	37,56	56,29	65,20	36,46	35,94	37,45	45,88	34,33	62,16
TiO2	0,77	0,59	1,14	0,05	0,00	0,17	0,00	0,78	0,07	0,07	0,04	1,55	2,78	0,00
Al2O3	19,97	32,7	19,32	19,91	20,29	19,82	26,55	17,59	20,20	19,93	20,45	33,49	18,59	23,43
FeO	5,28	1,26	21,44	34,27	32,97	34,49	0,75	6,05	35,53	36,67	36,89	1,45	21,50	0,12
MnO	0,02	0,08	0,07	0,62	0,37	1,46	0,13	0,11	1,15	2,32	1,50	0,02	0,01	0,00
MgO	1,96	0,77	8,21	3,47	4,32	3,15	0,00	1,39	4,03	3,00	3,06	0,79	7,19	0,00
CaO	0,97	0,04	0	3,91	3,47	3,68	8,59	0,39	1,53	1,36	1,49	0,00	0,00	4,89
Na2O	0,62	0,63	0,15	0,03	0,00	0,00	6,32	0,58	0,05	0,00	0,00	0,70	0,25	8,68
K2O	5,13	11,22	10,08	0,01	0,00	0,00	0,29	2,90				11,08	9,74	0,27
ZnO														
Sum	93,93	94,22	94,95	100,16	98,91	100,33	98,92	94,99	99,02	99,29	100,88	94,96	94,39	99,55
Si	59,90	6,35	5,36	6,08	6,04	6,04	2,56	66,33	5,95	5,92	6,02	6,18	5,36	2,77
Ti	–	0,06	0,13	0,01	0,00	0,02	0,00	–	0,01	0,01	0,00	0,16	0,33	0,00
Al	23,81	5,21	3,53	3,76	3,86	3,76	1,42	21,09	3,88	3,87	3,87	5,31	3,42	1,23
Fe	4,46	0,14	2,78	4,60	4,44	4,64	0,03	5,14	4,85	5,05	4,96	0,16	2,81	0,00
Mn	–	0,01	0,01	0,08	0,05	0,20	0,01	–	0,16	0,32	0,20	0,00	0,00	0,00
Mg	2,95	0,16	1,90	0,83	1,04	0,76	0,00	2,11	0,98	0,74	0,73	0,16	1,67	0,00
Ca	1,05	0,01	0,00	0,67	0,60	0,63	0,42	0,43	0,27	0,24	0,26	0,00	0,00	0,23
Na	1,21	0,17	0,05	0,01	0,00	0,00	0,56	1,15	0,02	0,00	0,00	0,18	0,08	0,75
K	6,62	1,94	2,00	0,00	0,00	0,00	0,02	3,76	0,00	0,00	0,00	1,90	1,94	0,02
O	167,89	22,00	22,00	24,00	24,00	24,00	8,00	174,43	24,00	24,00	24,00	22,00	22,00	8,00
Sum cations	100,00	14,04	15,76	16,04	16,03	16,05	5,01	100,00	16,11	16,14	16,04	14,05	15,61	5,00

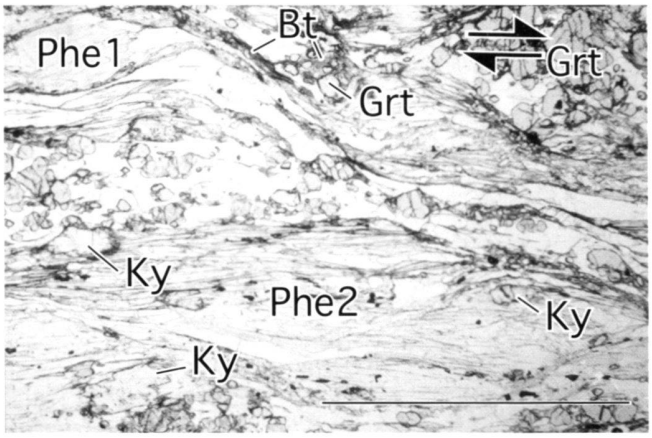

Fig. 9. Photomicrograph of sample TN212. Prekinematic phengite (Phe1) is embedded in a matrix of more or less recrystallized phengite (Phe2), Ky, Pg, Grt, and Qzt. Within the dextral shearband (= Top-NNE) biotite grows synkinematically. However, most of the biotite postdates the foliation in the section. Width of scalebar: 5 mm.

although folded by two phases (D2 and D3) the main foliations in this area form a great circle (stereoplot F in Fig. 4b). This clearly indicates that open D3 folds developed subparallel to a preexisting D2 planar and linear structure. Cobbold & Watkinson (1981) presented a possible explanation for such a behavior by proposing that an existing axial anisotropy of rocks may control the orientation of subsequent folding phases. Hence we believe that it is the pre-existing NW-SE-striking L2 and the N-S striking L1 streching lineations which may have induced the deflection of the D3 fold axes (see Fig. 4c). This hypothesis is in accordance with the observation that major D3 folds open towards north because the D3 fold axis orientations become progressively less suitable for accommodating N-S-directed shortening associated with the formation of the Southern Steep Belt.

Post-D3 structures

Subsequent to D3 folding the Southern Steep Belt was affected by considerable dextral strike slip movements which took place under greenschist facies conditions. North of the Insubric line these dextral movements produced distinct major shear zones and associated Riedel faults, of which the Paina fault is the most prominent one (Fumasoli 1974; Heitzmann 1974, 1975). In the Southern Steep Belt these dextral movements clearly overprint earlier steeply plunging lineations formed during backthrusting. Since the latter developed under conditions of the highest amphibolite facies, as indicated by synkinematic K-feldspar-sillimanite-bearing assemblages, we consider backthrusting across the Insubric mylonite belt to be coeval with D3. However, we correlate the above described post-D3 strike slip with brittle dextral overprint of the Insubric mylonites along the „Tonale fault" and related Riedel faults (Fumasoli 1974; Schmid et al. 1989).

Correlation of the metamorphic evolution with the deformation history

We now correlate mineral assemblages and associated P-T conditions with microstructures formed during the three major deformation phases outlined above. For each deformation phase D1-D3 one typical sample is presented in detail including geochemical results (Table 1). Each section starts with a description of the overall microstructural appearance of a particular deformation phase. These observations are derived from more than 200 samples of metapelites (Nagel 2000; Nagel et al. 2002). For the three selected samples equilibrium phase diagrams (De Capitani & Brown 1987; De Capitani 1994) are used to discuss P-T conditions and phase relations. Such diagrams provide stable assemblages, mineral modes, and compositions of solid solutions for a fixed bulk chemical composition in P-T space. We used the compositions of representative domains in thin sections to derive the input compositions presented in Table 1 (Nagel et al. 2002). We focussed on such phase diagrams, as they allow both the quantitative treatment of a single sample and the discussion of more general aspects of phase relations and their significance. The thermodynamic properties of minerals were taken from the database of Berman (1988, upgrade 1992) and slightly modified as presented in Nagel et al. (2002). All phases present in the database were considered in the calculations.

First deformation phase

The S1 foliation formed while garnet, quartz, phengite, paragonite, plagioclase biotite, and kyanite were stable as rock forming minerals in pelites and semipelites. Staurolite and chlorite commonly overgrow S1. Phengites aligned in S1 always show higher Si-contents when compared to postkinematic ones (see also Partzsch 1998; Löw 1987). In S1, synkinematic growth of biotite and plagioclase at the expense of garnet and white mica is frequently observed. However, the white mica/biotite ratio is generally high in S1 and there is no evidence for biotite or plagioclase to coexist with kyanite within S1 (Patzsch 1998; Meyre 1999b, Nagel 2002). Metabasic rocks equilibrated to garnet-bearing amphibolites during D1

We select sample TN212 from a locality in the Trescolmen zone, close to Cima de Gagela, for discussing D1 quantitatively. This specimen contains garnet, quartz, phengite, paragonite, kyanite and rutile which make up more than 95% of the thin-section (Fig. 9). In addition biotite, plagioclase, staurolite, ilmenite and zircon occur. The foliation is defined by quartz-ribbons and aligned large phengite and kyanite grains. Small amounts of phengite are also present as postkinematic fine grained aggregates. Kyanite displays slightly corroded grains with ragged grain boundaries and is clearly deformed during D1, as is indicated by kinking. Swarms of small garnets are mostly associated with boudinaged quartz domains. Paragonite is scarce and always associated with aligned phengite. The majority of biotite and plagioclase postdates S1, but they may also

appear during shear band formation in a late stage of D1 (Fig. 9). A few small staurolite crystals overgrow syn-D1 phengite. The chemical composition of phengites varies between 6.20 and 6.90 Si a.p.f.u. (Table1) with prekinematic porphyroblasts showing the highest Si-content. Even in direct contact to kyanite Si-contents up to 6.70 Si a.p.f.u. were measured. Perfectly aligned grains display lower Si-contents of 6.55–6.70 Si a.p.f.u. while in contact to biotite the Si-content of phengite is the lowest (6.20–6.45 Si a.p.f.u.). Garnet zonation is complex. In most grains two distinct shells with a relatively high Ca-content are present. The second Ca-rich generation represents the last growth-stage of garnet (Table 1). Later resorbtion of garnet is recorded by grain boundaries discordant to the internal zonation pattern and by a rise in abundance of Mn-content towards the grain boundary. This feature is best developed where plagioclase and biotite are present, which obviously grew at the expense of garnet. Thus, the entire zonation pattern predates the growths of biotite and plagioclase.

The phase diagram for sample TN212 (Fig. 10) predicts an oldest assemblage Grt + Qtz + Phe + Pg + Ky (1) to be stable above temperatures of 580 C° and pressures of 17 kbar. Phengites with Si-contents of 6.70 a.p.f.u. in this assemblage indicate pressures of around 22 kbar (see Si-contours in Fig. 10). Garnet-Phengite thermometry (Green & Hellman 1982) at grain boundaries between garnet and prekinematic high Si-phengite yields temperatures around 650 C°. These conditions (650 °C/ >20 kbar) agree well with P-T estimates of the pre-D1 high pressure stage in this area (Meyre et al. 1997; Meyre et al. 1999b). During decompression, phengite in assemblage 1 should become Al-richer through kyanite-consumption. For the present bulk composition kyanite is used up when phengite reaches a Si-content slightly less than 7.6 Si a.p.f.u. at pressures below 17 kbar. The resulting assemblage is Grt + Phe + Pg + Qtz (2). In sample TN212 kyanite of the high pressure assemblage 1 was corroded but a considerable amount still remained as a metastable phase in the rock. This prevented complete equilibration of phengite during decompression. We infer that eclogite facies conditions, preserved in pre-S1 phengite porphyroblasts, garnet, and kyanite predate S1. The Si-contents in large recrystallized phengite defining S1 are generally lower (6.50–6.70 Si a.p.f.u.) and indicate recrystallisation during decompression. Biotite and plagioclase only occur in shear bands during the final stages of D1 deformation at P-T conditions of 600–650 C° and 12 kbar (see assemblages 3 and 4 in Fig. 10). However, these P-T estimates regarding the final stages of D1 are only approximate because biotite probably grew at the expense of a not fully equilibrated phengite with a Si-content higher than predicted in figure 10. We emphazise that the observations in sample TN212 are not in conflict with our statement that kyanite does not coexist with biotite or plagioclase in S1 since kyanite is interpreted as a metastable high pressure relict. Pressures must certainly have exceeded 10 kbar during D1. This is indicated by postkinematic staurolite growth, at the expence of paragonite and garnet (Nagel et al. 2002), and additionally, by the synkinematic presence of garnet in amphibolites.

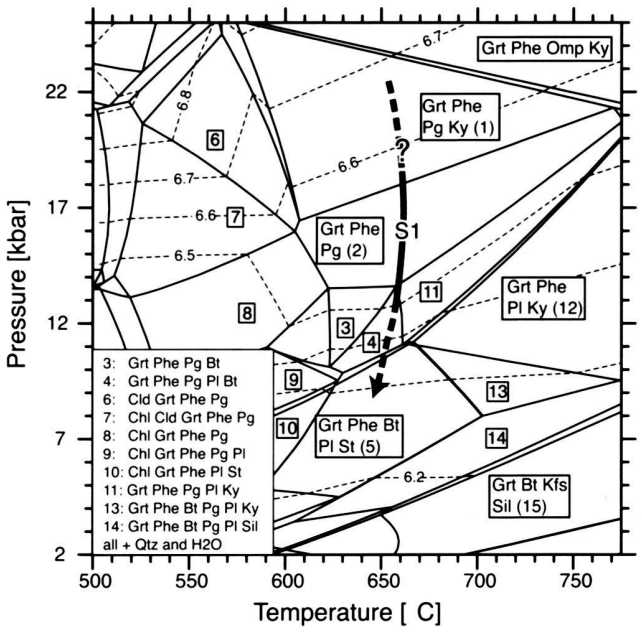

Fig. 10. Equilibrium phase diagram calculated for a representative domain of sample TN212 (Table 1). The diagram displays the predicted distribution of stable assemblages according to the thermodynamic properties of phases defined in the database (Berman, 1988, upgrade 92; ideal solution models for biotite, chlorite, and chloritoid; non ideal solution models for garnet (Berman 90), phengite (Massonne and Szpurka 97), plagioclase (Fuhrman & Lindsley 1988), staurolite (Nagel et al. 2002). Each field encloses the P-T space where a distinct assemblage is stable. Dashed lines represent contours of Si-content in phe (Si a.p.f.u.). The arrow indicates the supposed P-T path.

Assuming local equilibrium with kyanite, the postkinematic assemblage Grt + Qtz + Phe + Bt + Pl + Ky could be used to infer postkinematic P-T conditions with thermobarometry. INVEQ-thermobarometry (Gordon 1992) on such assemblages yields conditions of approximately 650 C°/10 kbar. However, all results have unsatisfying large uncertianties which may indicate that not even local equilibrium was achieved with kyanite at amphibolite facies conditions.

We conclude that although this sample exhibits significant disequilibrium, the equilibrium phase diagram predicts the observed mineral sequence in a correct order. Hence, it can be used to derive approximate P-T conditions in relation to the observed deformation structures. In the northern study area the foliation S1 formed during decompression at temperatures in excess of 600 C°. In metapelites this is indicated by two observations. Firstly, in kyanite-bearing assemblages Al-contents in phengite increased synkinematically through kyanite decomposition. Secondly, the onset of continuous white mica decomposition started during D1 (e.g. Ms + Grt = Bt + Al_2O_3 + Qtz) leading to the highest Al-contents in the remaining white mica. The resulting synkinematic succession of assemblages is Qtz + Grt + Phe + Pg ± Ky → Qtz + Grt + Phe + Pg → Qtz +

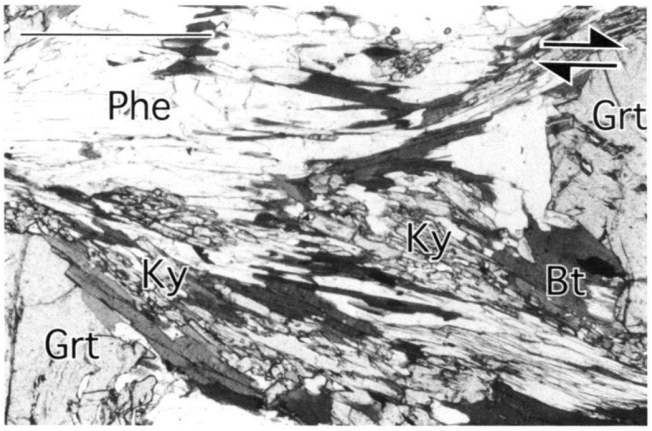

Fig. 11. Synkinematic growth of poikiloblastic kyanite and biotite at the expense of phengite and garnet during D2. Width of scalebar is 1 mm.

Grt + Phe + Pg ± Bt ± Pl. At the time D1 deformation ceased, P-T conditions of approximately 600–650 C° and 11–13 kbar were reached. S1 clearly postdates peak eclogite facies P-T conditions of 650 C°/ >20 kbar. The exact conditions at the onset of D1 deformation, however, could not be identified. Top-N shear bands have evolved during late stages of D1 deformation.

Second deformation phase D2

D2 microstructures are best preserved in the southwestern part of the study area. There, Grt + Qtz + Phe + Bt + Pl ± Ky is the stable assemblage in metapelites during the development of the S2 foliation. No paragonite was found any more and plagioclase appears as the only Na-bearing phase in all pelitic samples. However, further north, at Alp Calvarese, the complete paragonite breakdown seems to postdate D2 because staurolite and plagioclase, growing at the expense of paragonite and garnet, postdate the composite D1/D2 foliation found in that area (Nagel et al. 2002). Biotite and plagioclase are present regardless of rock-composition. The biotite/phengite ratio is higher than that found in S1. Phengite, though recrystallized, outlines D2 folds in sections perpendicular to D2 fold axes. Plagioclase often contains plenty of strongly corroded garnet fragments as inclusions. Biotite is commonly aligned in S2. A synkinematic modal increase of biotite and plagioclase is accompanied by decomposition of garnet and white mica. The Aluminium-release through this white mica breakdown often leads to the growth of kyanite in S2 (e.g. Ms + Grt = Bt + Ky + Qtz). In contrast to S1, kyanite coexists with biotite and plagioclase (Fig. 11). Staurolite and sillimanite postdate S2 in this southwestern area, though the microstructural position of staurolite in respect to S2 is locally ambiguous. The relation between kyanite (=syn-D2) and staurolite (=post-D2/post-kyanite) in the southern study area indicates that D2 took place on the high P-T side of the staurolite stability field (Nagel et al. 2002).

Sample TN349, selected for a quantitative discussion, contains the minerals garnet, kyanite, quartz, phengite, biotite, plagioclase, rutile, ilmenite, monazite, and zircon. The S2 foliation is defined by phengite and by aggregates of biotite. Abundant poikiloblastic kyanite is associated with biotite. These aggregates replace phengite in garnet-rich domains, preferentially in shear bands and pressure shadows of garnet (Fig. 11). Garnets display sigmoidal inclusion trails of quartz. At grain boundaries this internal schistosity is discordantly cut by S2. Although the sample comes from the Claro area (Bocchetta del Lago) located south of the sillimanite mineral zone boundary, the rock contains plenty of kyanite but lacks sillimanite, a common feature in this part of the Lepontine (see Todd & Engi 1997; Nagel et al. 2002). Both rutile and ilmenite are present in the matrix while inclusions in kyanite and plagioclase are dominantly rutile, hence in the matrix continuous rutile-breakdown (Grt + Rt = Ky + Ilm + Qtz) started. While phengite and biotite are chemically homogeneous, plagioclase shows increasing Ca-contents from core to rim. Garnets in this sample display also chemical evidence of considerable resorbtion. This is indicated by strongly increasing Mn-contents and increasing Fe/(Fe+Mg)-ratios right at the grain boundaries (Table 1), a common feature of garnets from this area.

The complete equilibrium phase diagram calculated for TN349 (Fig. 12) is similar to that calculated for TN212 (Fig. 10). The synkinematic assemblage Grt + Qtz + Phe + Bt + Pl + Ky (field 13 in Fig. 12) found in sample TN349 is stable at pressures around 10 kbar and temperatures in excess of 650 C°. Previous thermobarometric investigations yield conditions around 650 C° and 5-6 kbar in the Claro area, i.e. within the sillimanite stability field (Todd & Engi 1997). According to these authors, the equilibration of the samples postdates the S2 foliation. Hence their results are not in conflict with our P-T estimates for D2. The calculated modal amounts of phengite (Fig. 12a), biotite (Fig. 12b), garnet (Fig. 12c) indicate decompression associated with D2 as the observed decomposition of garnet and phengite in assemblage 13 is almost solely pressure dependent. Due to the chemical appearance of garnet, garnet-involving thermometers should not be applied to this sample (Spear & Parrish 1996) and we abandon determination of P-T conditions with thermobarometry.

We conclude that P-T conditions of approximately 650–700 °C and 10 kbar can be inferred for D2 in the southwestern part of the study area. Synkinematic growth of biotite, plagioclase and kyanite at the expense of phengite and garnet indicate decompression related to D2 deformation. Subsequent growth of staurolite and sillimanite postdates D2. Conditions at the onset of D2 deformation could not be determined directly, but the maximum pressure is limited by the well-constrained end of D1 deformation at around 12 kbar in the north of the study area. However, pressures could have been higher in the south at the start of D2 deformation.

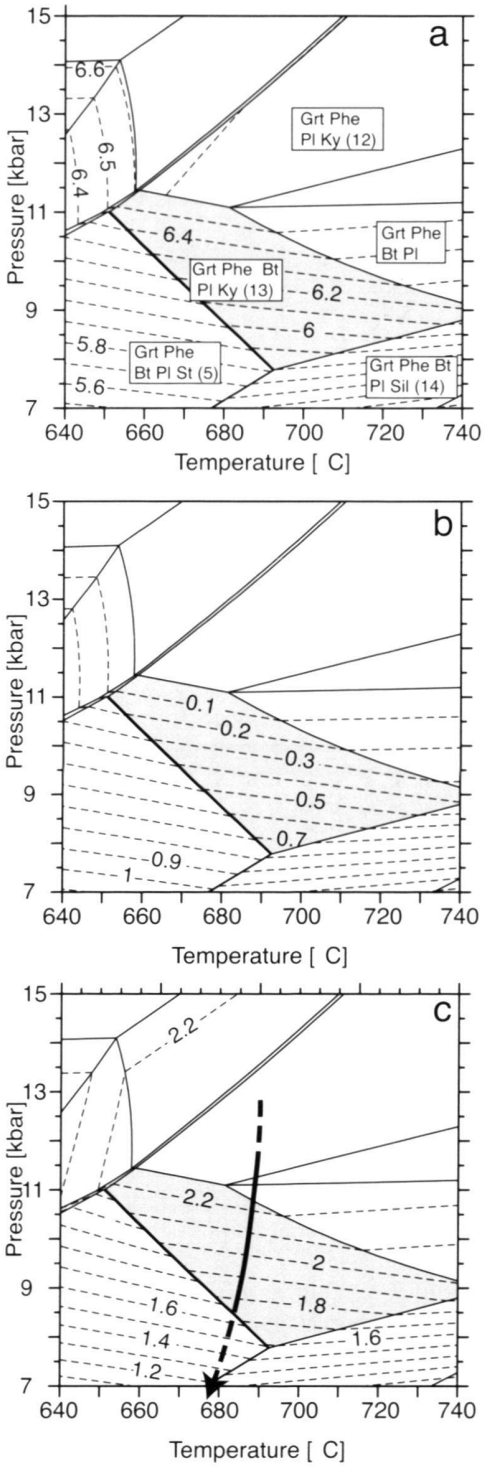

Fig. 12. Equilibrium phase diagrams calculated for the composition of a selected part of a thin section of sample TN349 (Table 1). The synkinematic assemblage 13 is shaded. Diagrams 13a-13c display the molar abundance of the rock forming minerals phengite (a), biotite (b), and garnet (c) for a composition normalized to 100 cations. These contours show that the observed synkinematic growth of biotite is almost purely pressure- dependent which indicates decompression during deformation.

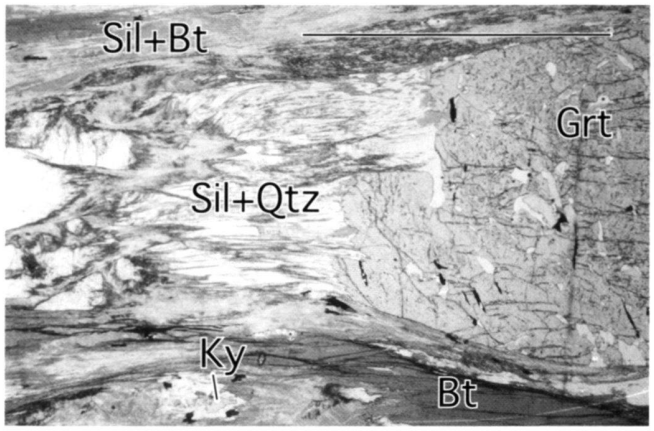

Fig. 13. Section parallel to D3 stretching lineation and fold axis. Synkinematic Qtz-Sil-aggregates indicate deformation in the sillimanite field. Phengite is almost completely decomposed to biotite in this sample (upper Val Grono). Width of scalebar is 5 mm.

Third deformation phase D3

Microstructures typical for D3 are found in the southeastern part of the study area (e.g. in the upper Val Grono) where D3 deformation is most intense and associated with the occurrence of migmatites in orthogneisses. Major phases in metapelites from that area are quartz, biotite, phengite, plagioclase, sillimanite, and garnet. North of the Paina marble phengite is still widely present. One sample containing K-feldspar and sillimanite has been found in the upper Val Grono (Jeker 2000) and further examples are reported from the literature (Hänny 1972; Thompson 1976). Within the Southern Steep Belt south of the Paina marble pelitic or semipelitic mylonites commonly show sillimanite + K-feldspar-bearing assemblages (see Fumasoli 1974). Except for one sample staurolite was not found in the matrix of rocks from this area. Kyanite is still widely preserved. However, in rocks affected by intense D3 deformation kyanite almost completely transformed to fibrolite (Fig. 13). Fibrolite is commonly intergrown with quartz or biotite, rarely also with phengite. In sections oriented parallel to the stretching lineation and D3 fold axis micas and especially quartz-sillimanite rods recrystallized synkinematically during D3 (Fig. 13). The alumosilicate associated with D2 is kyanite throughout the study area. Sillimanite-rich samples with only weak D3 deformation, e.g at Piz Cressim, show completely static equilibration. No significant growth of additional phases postdating D3 deformation was observed.

Sample TN236, taken from the upper Val Grono, displays the typical assemblages and microstructures described above. In contrast to other rocks in the area the sample contains large garnets up to 1 cm in size although phengite is almost completely transformed to biotite. Generally, minerals of this thin-section are only weakly zoned (Table 1).

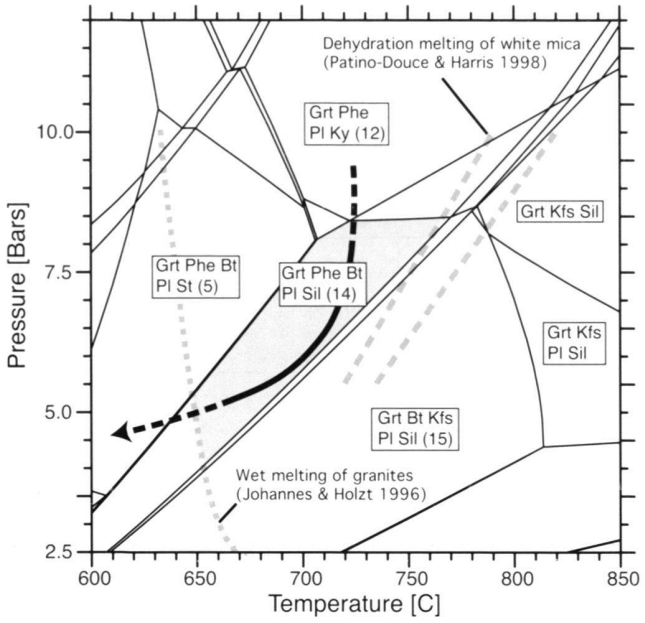

Fig. 14. Equilibrium phase diagram calculated for the composition of a of a selected part a thin section of sample TN236 (Table 1). Dotted line marks the wet solidus of granites (Johannes & Holtz 1996), dashed lines indicate experimentally determined wet melting of phegite (Patiño-Douce & Harris 1998).

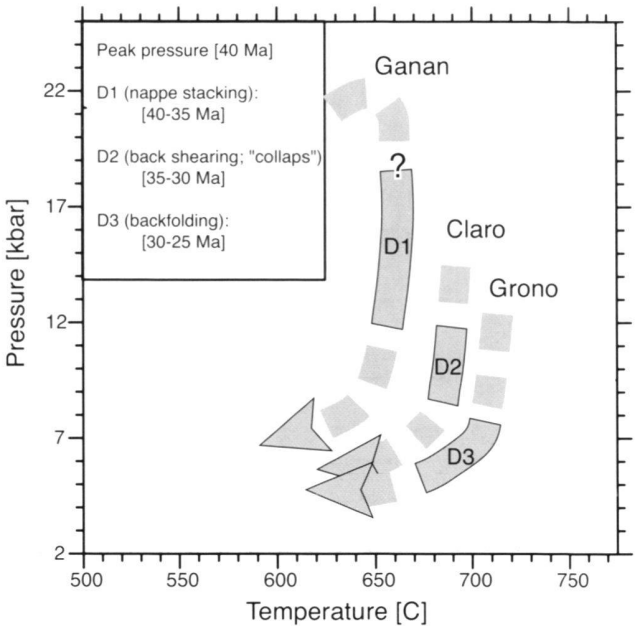

Fig. 15. P-T paths for the three localities discussed in the text and infered P-T conditions associated with a particular deformation phase at each locality. Pressures reflect progressive exhumation during D1-D3, while increasing temperatures are apparent and reflect different starting temperatures for the three localities.

P-T estimates related to D3 deformation can be derived accurately from the abundant assemblage Grt + Qtz + Bt + Pl + Phe + Sil (assemblage 14 of Fig. 14) and from the following field observations: presence of sillimanite and white mica, absence of staurolite in metapelites, and eutectic melting in orthogneiss. These constraints restrict the P-T conditions to 650–750 C° and 4–8 kbar (Fig. 14).

Todd & Engi (1997) derived conditions of > 650 C° and 5 kbar for this area using multi-equilibrium thermobarometry and we obtained the same result with our samples. It seems that chemical equilibration took place during D3 in the southeastern study area. Elsewhere, it can only be said that the thermobarometric results postdate D2. It is generally stated that the peak of amphibolite facies crystallization in the Lepontine occured between D2 and D3 (Ayrton & Ramsay 1974; Grujic & Mancktelow 1996). The southeastern part of our study area represents an exception from this observation since D3 deformation and crystallization is intense at a microscopic scale and since high temperature conditions still prevailed during D3 deformation. Todd and Engi (1997) also suggested that chemical equilibration in this specific area is younger than in the major part of the Lepontine dome because they obtained lower pressures compared to more northerly areas.

We conclude that the metamorphic conditions related to D3 in the southeastern part of the study area are around 650–700 C° and 4–6 kbar. Equilibration of mineral composition is concurrent with D3 since thermobarometric studies yield identical P-T conditions. This reequilibration of microstructures and mineral chemistry during D3 postdates the establishment of peak metamorphic conditions between D2 and D3 as observed in the central and northern parts of the Lepontine dome.

Overall evolution of metamorphic grade during deformation

The evolution of the metamorphic conditions during the three deformation phases is summarized in Fig. 15. Decreasing pressures and increasing temperatures are indicated by the three small portions of the P-T loops, obtained for D1, D2 and D3 in three different subareas. Note that these partial loops, and associated P-T conditions, were not observed within a single region of the study area. Moreover, portions of the P-T loops calculated for the particular specimens discussed earlier indicate different P-T evolutions for these different regions (Nagel et al. 2002). Consequently, these P-T estimates cannot be combined into a single P-T loop valid for the entire working area. In spite of this complication, the data presented above indicate that the pressure decreased during all deformation stages, recording progressive exhumation of the entire area during D1, D2 and D3. The temperature, however, cannot unequivocally be inferred to have increased or decreased during exhumation at any given locality. Instead, the shift of the three decompression loops towards higher temperatures (Fig. 15) is interpreted to result from the fact that the initial eclogite facies

temperatures have been higher in the south (Heinrich 1986). This interpretation is based on the observation that individual samples record isothermal decompression rather than heating (Nagel et al. 2002).

Time constraints and comparison with the tectono-metamorphic evolution of surrounding areas

We now discuss time constraints by comparing the structural and metamorphic evolution in the study area with that of surrounding regions: (1) the deeper Lower Penninic nappes of the Lepontine dome situated further to the west (e.g. Ayrton & Ramsay 1974; Grond et al. 1995; Grujic & Mancktelow 1996); (2) the northern and easternmost parts of the Adula nappe, including the Bergell pluton (e.g. Löw 1987; Partzsch 1998; Berger et al. 1996), and (3), the middle Penninic Tambo and Suretta nappes (e.g. Schreurs 1993; Baudin et al. 1993, Marquer et al 1994).

The characteristics of D1 to D3 in the study area correspond very well to deformation phases reported from the Maggia and Lebendun nappes (Grujic & Mancktelow 1996) or the Cima Lunga unit (Grond et al. 1995) further west. Problems arise concerning the correlation with some of the deformation phases found in the rest of Adula nappe, around the Bergell intrusion, and in the structurally higher Tambo and Suretta nappes where better absolute time constraints are available (e.g. discussion in Schmid et al. 1996).

Northwards and within the Adula nappe D1 of our study area corresponds in all respects to the Zapport phase (D2 in Löw 1987; D3 in Partzsch 1998), originally defined in the northern and middle Adula nappe. The onset of the Zapport phase (our D1) postdates peak eclogite conditions in the Adula nappe at about 40 Ma (Becker 1993; Gebauer 1996; Schmid et al. 1996). The next younger Leis phase (D3 of Löw 1987; D4 of Partzsch 1998) is associated with north-vergent folding and thrusting, which affect the northern parts of the Adula nappe. This phase is absent in most parts of our study area as it is completely dissimilar to the south-east directed shearing observed during our D2. This is in accordance with our observation that D2 overprint becomes weaker towards the north within the southern Adula nappe. Only at the northernmost rim of our study area south-vergent D2 folds and north-vergent Leis folds locally coexist, but unfortunately no direct overprinting structures and thus relations could be observed. The Leis phase of the northern Adula nappe indicates N-S compression and is interpreted to be contemporaneous with backfolding and backthrusting in the southern Lepontine area (e.g. Schmid et al. 1996; Partzsch 1998), hence contemporaneous with the D3 defined for our study area. Such a correlation implies that the Leis phase postdates D2 in the southern Adula nappe.

Based on structural and petrological observations Partzsch (1998) proposed that a distinct mylonite horizon at the contact between the northern Adula nappe and the sediments of the Soja Syncline is related to Leis phase north directed thrusting of the Adula nappe over the Simano nappe. According to our findings such a late northward directed thrusting of the Adula nappe during the Leis phase must have locally reworked an older nappe contact because the stacking of the Adula over Simano nappe is syn-D1 in our working area (i.e. syn-Zapport phase).

As we associate the formation of the Lower Penninic nappe stack with D1 (=Zapport phase), we conclude that this phase predates the onset of the formation of the Southern Steep Belt (Milnes 1974). The Bergell batholith, which is deformed by several large scale synmagmatic folds corresponding to the D3 folds of this study, started its ascent into an already existing steep zone at around 35 Ma (Berger et al. 1996, their Fig. 13; see also discussion in Steck & Hunziker 1994). This indicates that syn-D1 nappe stacking in our area pre-dates 35 Ma.

In the higher Tambo and Suretta nappes the so called Niemet-Beverin phase is infered to having been active between 35 and 30 Ma (e.g. Schmid et al. 1996; Weh & Froitzheim 2001). It definitely terminated before 30 Ma. This is indicated by the observation that the Bergell granodiorite truncates Niemet-Beverin structures (Turba normal fault of Nievergelt et al. 1996). The Niemet-Beverin phase (local D2) displays intense top-SE shearing, postdating top-N nappe stacking during the local D1 (Schreurs 1993; Baudin et al.1993; Ferrera phase of Schmid et al. 1996). On the basis of these kinematic similarity (top SE extensional shearing), we suggest that D2 observed in our working area corresponds to the 35–30 Ma old Niemet-Beverin phase, as does the geometrically similar D2 phase observed in the deeper lower Penninic nappes. Such a correlation corresponds to the model already proposed by Grujic & Mancktelow (1996).

We point out that pre-35 Ma nappe stacking in the Suretta and Tambo nappes (Ferrera phase) may have predated nappe stacking in the Lower Penninic nappes, since these middle Penninic units were accreted to the Austroalpine upper plate earlier (Schmid et al. 1996). Recent isotopic studies seem to confirm this concept. White micas defining the mylonitic S1 (Ferrera phase) foliation in a sample from the Suretta nappe yielded an age of 46 ± 5 Ma (Challandes 2000). In contrast, the Zapport phase in our study area must be considerably younger and certainly post-40 Ma as discussed previously.

Reliable constraints on the absolute timing of deformation events are available regarding the D3 backfolding phase (Cressim phase). Folds of this generation affect the base of the 30 Ma old granodiorite of the Bergell intrusion (von Blanckenburg 1992; Davidson et al. 1996; Berger et al. 1996) but are truncated by the 24.0 ±1.2 Ma old Novate granite (Liati et al. 2000). The D3 deformation corresponds to the Peschiera phase, the backfolding phase as defined by Berger et al. (1996) for the Bergell area.

In the study area, undeformed pegmatitic dykes dated 25.1 ±0.6 Ma (Gebauer 1996) intruded normal to D3 fold axes and postdate D3. The effects of post-25 Ma deformation are minor in the working area apart from the Forcola normal fault at the

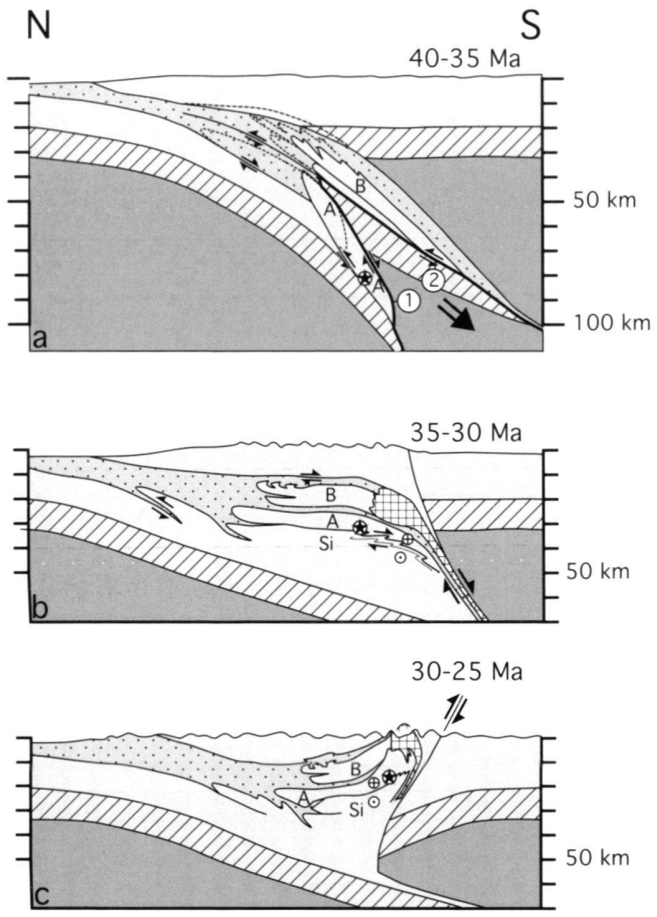

Fig. 16. Sketches illustrating the major stages of exhumation for the Adula nappe (modified after Schmid et al. 1996). Stars indicate the position of the base of the Adula nappe within our working area after each step during progressive exhumation. SI: Simano nappe; A: Adula nappe; B: Briançonnais units (Tambo and Suretta nappe).

(a) D1 deformation (Zapport phase) and exhumation at 40 to 35 Ma ago. During the earlier and main stage of the Zapport phase ascent of the Adula nappe within the subduction channel exhumes the Adula nappe from 22 to 12 kbar (stippled outlines of Adula nappe). Note that top-S shearing at the top of the Adula nappe must have occurred between the Adula nappe and former lower crustal and mantle underpinnings of the Suretta and Tambo nappes (top-S shear zone labelled 1). During the closing stages of Zapport phase these underpinnings became completely subducted ("blind extensional allochthon" according to Michard et al. 1993). Note that this mechanism results in a substantial amount of vertical shortening. At the same time the Tambo and Suretta upper crustal flakes were emplaced onto the Adula nappe (stippled outlines of Tambo and Suretta nappes), overprinting the former top-S shear zone in the roof of the Adula nappe by top-N shearing (top-N shear zone labelled 2).

(b) Situation of the geometry at the end extensional unroofing (from 12 to 8 kb) by gravitational collapse (35–30 Ma old Niemet-Beverin phase), associated with top SE shearing near the Simano-Adula nappe boundary (our D2) and near the base of the orogenic lid (Turba normal fault).

(d) Situation after the third stage of exhumation (from 8 to 4 kb) by erosion, caused by backfolding and backthrusting between 30 and 25 Ma ago.

Adula-Tambo nappe boundary (Meyre et al. 1999a) and dextral shearing within the Paina marble mylonite (Heitzmann 1987). However, backthrusting within the Insubric mylonite belt (Schmid et al. 1989), although associated with greenschist and subgreenschist facies conditions, is syn-D3 (see discussion in Berger et al. 1996) and hence directly related to syn-D3 exhumation. Post-D3 (post 25 Ma) deformation is restricted to dextral strike slip movements at the Insubric line.

Conclusions

Pervasive ductile deformation in the study area becomes progressively younger from north to south. Microstructural and petrological evidence shows that penetrative structures that developed during our D1 (Zapport) phase are associated with decompression under relatively high pressures (22–12 kbar, see also Partzsch 1998). Shear senses (top-N shearing) and structural evidence indicate that the Zapport phase is related to nappe stacking. Hence, exhumation by extensional unroofing in the sense of normal faulting and/or overall crustal thinning (gravitational spreading) is ruled out for this first and very fast stage of exhumation of the Adula nappe between 40 and 35 Ma (7 mm/a, corresponding to decompression by 10 kbar within 5 Ma). Since erosion in combination with thrusting cannot explain the jump to lower peak pressures across the top of the Adula nappe (Tambo-Suretta nappes) we can only envisage exhumation within the subduction channel by active „extrusion" or buoyant ascent of the Adula nappe within the subduction channel (return of a „pip" or „continental sheet" according to Wheeler 1991, his Figure 13; also see Chemenda et al. 1995).

This interpretation is in accordance with the observation that underthrusting of the Adula nappe with the downgoing plate predates Zapport phase nappe stacking (see pre-Zapport phases discussed by Löw 1987; Partzsch 1998; Meyre et al. 1997, Meyre 1998). Ongoing top-N underthrusting of the European foreland in the deeper lower Penninic and Helvetic nappes (i.e. Simano nappe), as proposed by Schmid et al. (1996) during D1/Zapport phase nappe stacking leads to increasing pressures and temperatures within those lower tectonic units. Contemporaneous decompression in the Adula nappe is caused by the differential ascent of this nappe within the subduction channel. Serious problemes arise in regard to the top-N shearing also observed at the top of the Adula nappe (Partzsch 1998; Meyre 1998; Meyre et al. 1999b and own observations). The top-S shearing, necessary for differential ascent of the Adula nappe in respect to the Tambo nappe in its hangingwall, has neither yet been observed near the roof of the Adula nappe nor within the Misox zone. This rises the question about the exact nature of the P-T evolution during the Zapport phase top-N shearing observed near the top of the Adula nappe. Lacking a viable alternative model for exhumation by ascent within the subduction channel in order to explain decompression during the Zapport phase we propose the following scenario illustrated in figure 16a. Top-N shearing

near the top of the Adula nappe is only related to the closing stages of Zapport phase deformation (top-N shear zone 2 in Fig. 16a) and is associated with late stage north directed thrusting of the Tambo nappe. This late stage top-N thrusting follows earlier decompression associated with top-S shearing (top-S shear zone 1 in Fig. 16a), and it completely overprints former top-S shear sense indicators. This earlier stage combines ascent of the Adula nappe within the subduction zone with vertical thinning due to the complete subduction of the lithospheric mantle of the Tambo and Suretta nappes ("blind extensional allochthon" of Michard et al. 1993). Interestingly, substantial decompression during top-N to top-W nappe stacking has also been reported from other eclogitic units (Dora Maira, e.g. Wheeler 1991; M. Rosa, e.g. Keller & Schmid 2001).

Strain intensity during D2, corresponding to the 35-30 Ma old Niemet Beverin phase, increases southward and progressively overprints S1. This D2 is accompanied by the formation of a new axial planar foliation S2, a rotation of the finite stretching lineation from a N-S into a NW-SE orientation, and a reversal of the sense of shearing from top-N to top-SE. This Niemet-Beverin phase represents the only stage of exhumation (from 12 to 8 kb) which has to be related to extensional unroofing by gravitational spreading and/or orogen-oblique stretch. We propose that, between 35 and 30 Ma, the area adjacent to the Southern Steep Belt was active as a south dipping fault zone with a normal sense of shear during D2. Collapse of the overthickened nappe pile most likely caused this extension (Fig. 16b).

The synmagmatic and synmigmatitic D3 backfolding phase (Cressim phase) is active during in the 30–25 Ma time interval. It is particularly well developed in the southeasternmost part of the study area, where E-W-trending, tight D3 folds are associated with a stretching lineation L3, oriented parallel to fold axes. Further towards the N strain intensity decreases while the axes of major and minor D3 folds swing towards a NW-SE to N-S orientation, pre-determined by the orientation of pre-existing L2 and L1 lineations. Backthrusting within the Insubric mylonite belt (Schmid et al. 1989) coupled with rapid erosion seems to be the dominant exhumation mechanism (from 8 to 4–5 kb) during D3 (Fig. 16c).

Finally, we conclude that, although rapid exhumation is associated with the three major ductile deformation phases D1-D3, the locus of penetrative deformation migrated southwards. The mechanisms of exhumation changed during these three stages of the exhumation history.

Acknowledgements

We thank Matthias Damo, Andreas Frischbutter, Oliver Jeker, and Beat Niederberger who provided data from their diploma theses which is presented in Fig. 4 and 5. Intense discussions with Neil Mancktelow are gratefully acknowledged. Reviews of Peter Tropper, Alexander Proyer, and Kurt Krenn are greatly acknowledged. This study is a part of the PhD thesis of Thorsten Nagel. At the same time it is the result of a project sponsered by the Swiss National Science Foundation (grants 20-45270.95 and 20-53636.98). This study would not have been possible without the support of the late Martin Frey.

REFERENCES

AYRTON, S. N. & RAMSAY, J. G. 1974: Tectonic and metamorphic events in the Alps. Schweiz. Mineral. Petrogr. Mitt. 54, 609–639.

BAUDIN, T., MARQUER, D. & PERSOZ, F. 1993: Basement-cover relationships in the Tambo nappe (Central Alps, Switzerland): geometry, structure and kinematics. J. Struct. Geology 15, 543–553.

BECKER, H. 1993: Garnet peridotite and eclogite Sm-Nd ages from the Lepontine Dome (Swiss Alps): new evidence for Eocene high pressure in the central Alps. Geology 21, 599–602.

BELLIN, J. 1929: Zur Geologie des östlichen Misox zwischen Valle della Forcola und Val Leggia. Diss. Univ. Zürich, Switzerland

BERGER, A., ROSENBERG, C. & SCHMID, S.M. 1996: Ascent, emplacement and exhumation of the Bergell pluton within the Southern Steep Belt of the Central Alps. Schweiz. Mineral. Petrogr. Mitt. 76, 357–382.

BERMAN, R. G. 1988: Internally-consistent thermodynamic data for minerals in the system Na2O-K2O-CaO-FeO-Fe2O3-Al2O3-SiO2-TiO2-H2O-CO2. J. Petrology 29, 445–522.

– 1990: Mixing properties of Ca-Mg-Fe-Mn garnets. Amer. Mineralogist 75, 328–344.

BLATTNER, P. 1965: Ein anatektisches Gneissmassiv zwischen Valle Bodengo und Valle di Livo (Prov. Sondrio und Como). Schweiz. Mineral. Petrogr. Mitt. 45, 973–1071.

BRUGGMANN, H.O. 1965: Geologie und Petrographie der südlichen Misox. Diss. Univ. Zürich, Switzerland

CHALLANDES, N. 2000: Comportement des systèmes isotopiques 39Ar-40Ar et Rb-Sr dans les zonesde cisaillement: Exemples du massif de l'Aar (Massifs cristallins externes) et de la nappe de Suretta (Alpes centrales suisses). Ph. D. thesis, Univ. Neuchâtel, Switzerland

CHEMENDA, A.I., MATTAUER, M., MALAVIEILLE, J. & BOKUN, A.N. 1995: A mechanism for syn-collisional rock exhumation and associated normal faulting: results from physical modelling. Earth and Planet. Sci. Lett. 132, 225–232.

COBBOLD, P.R. & WATKINSON, A.J. 1981: Bending anisotropy: a mechanical constraint on the orientation of fold axes in a anisotropic medium. Tectonophysics 72, 1–10.

CODONI, A. 1982: Geologia e Petrografia della Regione del Pizzo di Claro. Diss. Univ. Zürich, Switzerland.

DAMO, M. 2000: Geologie und Petrographie des Cessim (Val d'Arbola, Misox). Unpublished diploma thesis, Univ. Basel, Switzerland, 71 p.

DAVIDSON, C., ROSENBERG, C. & SCHMID, S.M. 1996: Synmagmatic folding of the base of the Bergell pluton, Central Alps. Tectonophysics 265, 213–238.

DE CAPITANI, C. 1994: Gleichgewichts-Phasendiagramme: Theorie und Software. Beih. Europ. J. Mineralogy, 72. Jahrestagung der Deutschen Mineralogischen Gesellschaft 6, 48.

DE CAPITANI, C. & BROWN, T.H. 1987: The computation of chemical equilibrium in complex systems containing non ideal solutions. Geochim. Cosmochimi. Acta 51, 2639–2652.

FRISCHBUTTER, A. 2000: Strukturgeologische Analyse im Bereich der südlichen Grenzzone zwischen Simano- und Adula-Decke (südliches Valle Mesolcina, Graubünden, CH). Unpubl. diploma work, Univ. Freiburg, Germany.

FRISCHKNECHT, G 1923: in JENNY, H., FRISCHKNECHT, G. & KOPP, J. 1923: Geologie der Adula. Beitr. Geol. Karte Schweiz N.F. 51, 123.

FROITZHEIM, N., SCHMID, S.M. & FREY, M. 1996: Mesozoic paleogeograhy and the timing of eclogite-facies metamorphism in the alps: A working hypothesis. Eclogae Geol. Helv. 89, 81–110.

FUMASOLI, M.W. 1974: Geologie des Gebietes nördlich und südlich der Jorio-Tonale-Linie im Westen von Gravedone (Como, Italia). Diss. Univ. Zürich, Switzerland.

FUHRMAN, M. L. & LINDSLEY, D. H. 1988: Ternary-feldspar modeling and thermometry. Amer. Mineralogist 73, 201–216.

GEBAUER, D. 1996: A P-T-t-d path for a (ultra?-) high-pressure ultramafic/mafic rock association and their felsic country-rocks based on SHRIMP-dating of magmatic and metamorphic Zirkon domains. Example: Alpe Arami (Central Swiss Alps). Geophysical Monograph Series, Special AGU-monograph dedicated to Profs. Tilton and Tatsumoto: Earth Processes: reading the Isotopic code. 95, 307–329.

GORDON, T. 1992: Generalized thermobarometry; solution of the inverse chemical equilibrium problem using data for individual species. Geochimi. Cosmochimi. Acta 56, 1793–1800.

GREEN, T. H., & P. L. Hellman 1982: Fe-Mg partitioning between coexisting garnet and phengite at high pressure, and comments on a garnet-phengite thermometer. Lithos 15, 253–266.

GROND, F., WAHL, F. & PFIFFNER, M. 1995: Mehrphasige alpine Deformation und Metamorphose in der nördlichen Cima-Lunga-Einheit, Zentralalpen (Schweiz). Schweiz. Mineral. Petrogra. Mitt. 75, 371–386.

GRUJIC, D. & MANCKTELOW, N. 1996: Structure of the northern Maggia and Lebendun Nappes, Central Alps. Switzerland: Eclogae Geol. Helv. 89, 461–504.

HANNY, R. 1972: Das Migmatitgebiet in der Valle Bodengo. Beitr. Geol. Karte Schweiz N.F. 145.

HEIM, A. 1891: Geologie der Hochalpen zwischen Reuss und Rhein. Beitr. Geol. Karte Schweiz 25.

HEINRICH, C.A. 1986: Eclogite facies regional metamorphism of hydrous mafic rocks in the Central Alpine Adula nappe. J. Petrology 27, 123–154.

HEITZMANN, P. 1974: Die „Wurzelzone" zwischen Valle di Liviound Lago di Mezzola (Prov. di Como, Italia), Ph.D. thesis, ETH Zürich, Switzerland.

– 1975: Zur Metamorphose und Tektonik im südöstlichen Teil der Lepontinischen Alpen. Schweiz. Mineral. Petrogr. Mitt. 55, 467–522.

HEITZMANN, P. 1987: Calcite mylonites in the Central Alpine „root zone". Tectonophysics 135, 207–215.

HEYDWEILER, E. 1918: Geologische und Morphologische Untersuchungen in der Gegend des St. Bernadinpasses. Eclogae Geol. Helv. 15, 149–296.

HUBER, R. K. 1993: Ein Beitrag zur Geologie des südlichen Misox. Unpubl. diploma thesis, ETH-Zürich, Switzerland.

JEKER, O. 2000: Strukturen umd Metamorphose in der oberen Val Grono (südl. Adula), Teil 1. Unpubl. diploma thesis, Univ. Basel, Switzerland, 88 p.

JENNY, H. 1923: in JENNY, H., FRISCHKNECHT, G. & KOPP, J. 1923: Geologie der Adula. Beitr. Geol. Karte Schweiz N.F. 51, 123.

JENNY, H., FRISCHKNECHT, G. & KOPP, J. 1923: Geologie der Adula. Beitr. Geol. Karte Schweiz N.F. 51, 123.

JOHANNES, W. & HOLTZ, F. 1996: Petrogenesis and experimental petrology of granitic rocks. Springer Verlag, 335 p.

KELLER, L. & SCHMID, S.M., 2001: On the kinematics of shearing near the top of the Monte Rosa nappe and the nature of the Furgg zone in Val Loranco (Antrona valley, N. Italy): tectono-metamorphic and paleogeographical consequencees. Schweiz. Mineral. Petrogr. Mitt. 81, 347–367.

KLEIN, H.H. 1976: Metamorphose von Peliten zwischen Rheinwaldhorn und Pizzo Paglia (Adula- und Simano-Decke). Schweiz. Mineral. Petrogr. Mitt. 56, 457–479.

KNOBLAUCH, P., REINHARD, M. & KÜNDIG, E. 1939: Geologischer Atlas der Schweiz 1:25000. 516 Iorio. Geol. Kommission der S. N. G.

KOPP, J. 1922: Zur Tektonik des Pizzo di Claro und der Wurzelzone im unteren Misox. Eclogae Geol. Helv. 17, 555–562.

– 1923a: Bau und Abgrenzung der Simano- und Aduladecke im südöstlichen Misox. Eclogae Geol. Helv. 18, 259–265.

– 1923b: in JENNY, H., FRISCHKNECHT, G. & KOPP, J. 1923: Geologie der Adula. Beitr. Geol. Karte Schweiz N.F. 51, 123.

KÜNDIG, E. 1926: Beiträge zur Geologie und Petrographie der Gebirgskette zwischen Val Calanca und Misox. Schweiz. Mineral. Petrogr. Mitt. 4, 1–99.

LIATI, A., GEBAUER, D. & FANNIMG, M. 2000: U-Pb SHRIMP-dating of zircon from the Novate granite (Bergell, Central Alps): evidence for Oligocene-Miocene magmatism, Jurassic-Cretaceous continental rifting and opening of the Valais trough. Schweiz. Mineral. Petrogr. Mitt. 80, 305–316.

LÖW, S. 1987: Die tektono-metamorphe Entwicklung der Adula-Decke. Beitr. Geol. Karte Schweiz NF 161.

LUGEON, M. 1901: Les grandes nappes de recouvrement des Alpes du Chablais et de la Suisse. Bull. Soc. géol. France IV 1, 723–825.

MARQUER, D., BAUDIN, T. PEUCAT, J.-J. & PERSOZ, F. 1994: Rb-Sr mica ages in the Alpine shear zones of the Truzzo granite: timing of the tertiary Alpine P-T-deformations in the Tambo nappe (Central Alps, Switzerland). Eclogae Geol. Helv. 87, 225–239.

MASSONNE, H.-J. & SZPURKA, Z. 1997: Thermodynamic properties of white micas on the basis of high-pressure experiments in the systems K2O-MgO-Al2O3-SiO2-H2O and K2O-FeO-Al2O3-SiO2-H2O. Lithos 41, 229–250.

MEYRE, C., DE CAPITANI, C.& PARTSCH, J.H. 1997: A ternary solid solution model for omphacite and its application to geothermobarometry of eclogites from the Middle Adula nappe (Central Alps, Switzerland). J. Metamorphic Geology 15, 687–700.

MEYRE, C. 1998: High-pressure metamorphism and deformation of the middle Adula nappe. Ph. D. thesis, Univ. Basel, Switzerland.

MEYRE, C., MARQUER, D., SCHMID, S.M. & L. CIANCALEONI 1999a: Syn-orogenic extension along the Forcola fault. Eclogae Geol. Helv. 91, 409–420.

MEYRE, C., DE CAPITANI, C., ZACK, T. & FREY M. 1999b: Petrology of high-pressure metapelites from the Adula nappe (Central Alps, Switzerland). J. Petrology 40, 199–213.

MICHARD, A., CHOPIN, C. & HENRY, C. 1993. Compression versus extension in the exhumation of the Dora-Maira coesite-bearing unit, Western Alps, Italy. Tectonophysics 221, 173–193.

MILNES, A.G. 1974, Structure of the Pennine Zone (Central Alps): A new working hypothesis. Bull. Geol. Soci. America 85, 1727–1732.

– 1978: Structural Zones and Continental Collision, Central Alps. Tectonophysics 47, 369–392.

NAGEL, T 2000: Metamorphic and structural history of the southern Adula nappe (Graubünden, Switzerland). Ph.D. thesis, Univ. Basel, Switzerland.

NAGEL, T., DE CAPITANI, C. & FREY, M. 2002: Isograds and P-T evolution in the eastern Lepontine Alps (Graubünden, Switzerland). J. Metamorphic Geology 20, 309–324.

NIEDERBERGER, B. 2000: Strukturen umd Metamorphose in der oberen Val Grono (südl. Adula), Teil 2. Unpubl. diploma thesis, Univ. Basel, Switzerland, 83 p.

NIEVERGELT, P., LINIGER, M., FROITZHEIM, N. & FERREIRO-MAHLMANN, R. 1996: Early to mid Tertiary crustal extension in the Central Alps: The Turba mylonite zne (Eastern Switzerland). Tectonics 15, 329–340.

NIGGLI, E. & NIGGLI, C.R. 1965: Karten der Verbreitung einiger Mineralien der alpidischen Metamorphose in den Schweizer Alpen (Stilpnomelan, Alkali-Amphibol, Chloritoid, Staurolith, Disthen, Sillimanit). Eclogae Geol. Helv. 58, 335–368.

NIMIS, P. & TROMMSDORFF, V. 2001: Revised thermobarometry of Alpe Arami and other garnet peridotites from the Central Alps. J. Petrology 42, 103–115

PARTZSCH, J.H. 1998: The tectono-metamorphic evolution of the middle Adula nappe, Central Alps, Switzerland. Ph.D. thesis, Univ., Basel, Switzerland.

PLAS, A. 1992: Pertografia e Geologia Strutturale della Zona di Roveredo-San Vittore bassa Val Mesolcina, Gr/Ch. Unpubl. diploma thesis, ETH-Zürich, Switzerland.

PATIÑO-DOUCE, A. & HARRIS, N. 1998: Experimental Constraints on Himalayan Anatexis. J. Petrology 39, 689–710.

PREISWERK, H. 1921: Die zwei Deckenkulminationen Tosa-Tessin und die Tessiner Querfalte. Eclogae Geol. Helv. 16, 485–496.

RAMSAY, J.G. & HUBER, M.I. 1987: Modern Structural Geology, Volume 2: Folds and Fractures. London, Academic Press.

ROLLE, F. 1881: Das südwestliche Graubünden und das nordöstliche Tessin. Beitr. Geol. Karte Schweiz 23.

RÜTI, R. 2001: Tectono-metamorphic evolution of the Simano-Adula nappe boundary, Central Alps, Switzerland. Schweiz. Mineral. Petrogr. Mitt. 81, 115–129.

SCHARDT, H. 1898: Les régions exotiques du versant nord des Alpes Suisses. Bull. Soc. Vaud. Sci. Nat. 34/128, 113–219.

SCHMID, S. M., H. R. AEBLI, F. HELLER & A. ZINGG, 1989: The role of the Periadriatic Line in the tectonic evolution of the Alps. In: M. P. Coward, D. Dietrich & R. G. Park, eds., Alpine Tectonics, Geological Society of London, p. 153–171.

SCHMID, S.M., PFIFFNER, O.A., SCHÖNBORN, G., FROITZHEIM, N. & KISSLING, E. 1996: Geophysical-geological transect and tectonic evolution of the Swiss-Italian Alps. Tectonics 15, 1036–1064.

SCHREURS, G. 1993: Structural analysis of the Schamps nappes and adjacent tectonic units: implications for the orogenic evolution of the Penninic zone in eastern Switzerland. Bull. Soc. Géol. France 164, 415–435.

SPEAR, F. S., & PARRISH , R. R., 1996: Petrology and cooling rates of the Valhalla Complex, British Columbia, Canada. J Petrology 37, 733–765.

SPICHER, A. 1980: Tektonische Karte der Schweiz (1:500000): Schweiz. Geol. Komm.

SPILLMANN, P. 1993: Die Geologie des penninisch-ostalpinen Grenzbereichs im südlichen Berninagebirge. Ph.D. Thesis, ETH Zürich, Switzerland.

STAUB, R. 1916: Zur Tektonik der südöstlichen Schweitzeralpen. Mit tektonischer Übersichtskarte. Beitr. geol. Karte Schweiz, NF 46.

STAUB, W. 1930, Geologische Wandkarte der Schweiz. Kümmerli und Frey.

STECK, A. 1999: The Maggia cross-fold. Eclogae Geol. Helv. 91, 333–344.

STECK, A. & HUNZIKER, J. 1994: The Tertiary structural and thermal evolution of the Central Alps. Compressional and extensional structures in an orogenic belt. Tectonophysics 238, 229–254.

STEINMANN, M. & STILLE, P. 1999: Geochemical evidence for the nature of the crust beneath the eastern north penninic basin of the Mesozoic Thetys ocean. Geol. Rdsch. 87, 633–643.

STRASSER, E. 1928: Geologie der Pizzo die Claro- Torrone Alto-Kette sowie der Penninischen Wurzelzone zwischen Val Calanca und Tessintal. Ph. D. thesis, Universität Zürich, Switzerland

STUDER, B. & ESCHER, A. 1853: Carte géologique de la Suisse, 1:380,000; 1st sheet. Wurster & Co.

STÜNITZ, H. 1991: Folding and shear deformation in quartzites, infered from crystallographic preferred orientation and shape fabrics. J. Structural Geol. 13, 71–86.

THOMPSON, H.P. 1976: Isograd patterns and pressure-temperature distribution during regional metamorphism. Contr. Mineral. Petrol. 57, 277–295.

TODD, C.S. & M. ENGI 1997: Metamorphic field gradients in the Central Alps. J. Metamorphic Geology 15, 513–530.

VAN DER PLAS, L. 1959: Petrology of the northern Adula region, Switzerland (with particular reference to the glaucophane-bearing rocks). Leidse Geol. Meded. 24, 413–603.

VON BLANCKENBURG, F. 1992: Combined high-precision chronometry and geochemical tracing using accessory minerals: applied to the Central-Alpine Bergell intrusion (central Europe). Chemical Geology 100, 19–40.

WEBER, W. 1966: Zur Geologie zwischen Chiavenna und Mesocco: Ph.D. thesis, ETH-Zürich, Switzerland.

WHEELER, J. 1991. Structural evolution of a subducted continental sliver: the northern Dora Maira massif, Italian Alps. J. Geol. Soc. (London) 148, 1101–1113.

WEH, M. & FROITZHEIM, N. 2001: Penninic cover nappes in the Prättigau halfwindow (Eastern Switzerland): Structure and tectonic evolution. Eclogae Geol. Helv. 94, 237–252.

WENK, E. 1955: Eine Strukturkarte der Tessineralpen. Schweiz. Mineral. Petrogr. Mitt. 35, 311–319.

WILCKENS, O. 1907: Über den Bau des nordöstlichen Adulagebirges. Cbl. Mineral. 1907, 341–348.

Manuscript received March 6, 2002
Revision accepted July 31, 2002